Radiology

Fleischner Society: Glossary of Terms for Thoracic Imaging[1]

David M. Hansell, MD, FRCP, FRCR
Alexander A. Bankier, MD
Heber MacMahon, MB, BCh, BAO
Theresa C. McLoud, MD
Nestor L. Müller, MD, PhD
Jacques Remy, MD

Members of the Fleischner Society compiled a glossary of terms for thoracic imaging that replaces previous glossaries published in 1984 and 1996 for thoracic radiography and computed tomography (CT), respectively. The need to update the previous versions came from the recognition that new words have emerged, others have become obsolete, and the meaning of some terms has changed. Brief descriptions of some diseases are included, and pictorial examples (chest radiographs and CT scans) are provided for the majority of terms.

© RSNA, 2008

© RSNA, 2008

The present glossary is the third prepared by members of the Fleischner Society and replaces the glossaries of terms for thoracic radiology (1) and CT (2), respectively. The impetus to combine and update the previous versions came from the recognition that with the recent developments in imaging new words have arrived, others have become obsolete, and the meaning of some terms has changed. The intention of this latest glossary is not to be exhaustive but to concentrate on those terms whose meaning may be problematic. Terms and techniques not used exclusively in thoracic imaging are not included.

Two new features are the inclusion of brief descriptions of the idiopathic interstitial pneumonias (IIPs) and pictorial examples (chest radiographs and computed tomographic [CT] scans) for the majority of terms. The decision to include vignettes of the IIPs (but not other pathologic entities) was based on the perception that, despite the recent scrutiny and reclassification, the IIPs remain a confusing group of diseases. We trust that the illustrations enhance, but do not distract from, the definitions. In this context, the figures should be regarded as of less importance than the text—they are merely examples and should not be taken as representing the full range of possible imaging appearances (which may be found in the references provided in this glossary or in comprehensive textbooks).

We hope that this glossary of terms will be helpful, and it is presented in the spirit of the sentiment of Edward J. Huth that "scientific writing calls for precision as much in naming things and concepts as in presenting data" (3). It is right to repeat the request with which the last Fleischner Society glossary closed: "[U]se of words is inherently controversial and we are pleased to invite readers to offer improvements to our definitions" (2).

Glossary

acinus

Anatomy.—The acinus is a structural unit of the lung distal to a terminal bronchiole and is supplied by first-order respiratory bronchioles; it contains alveolar ducts and alveoli. It is the largest unit in which all airways participate in gas exchange and is approximately 6–10 mm in diameter. One secondary pulmonary lobule contains between three and 25 acini (4).

Radiographs and CT scans.—Individual normal acini are not visible, but acinar arteries can occasionally be identified on thin-section CT scans. Accumulation of pathologic material in acini may be seen as poorly defined nodular opacities on chest radiographs and thin-section CT images. (See also *nodules.*)
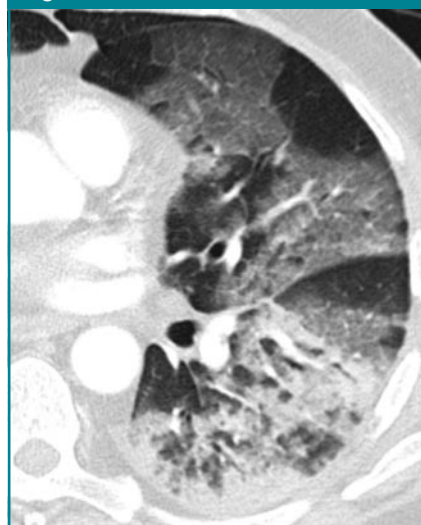

Figure 1: Transverse CT scan in a patient with acute interstitial pneumonia.

acute interstitial pneumonia, or AIP

Pathology.—The term *acute interstitial pneumonia* is reserved for diffuse alveolar damage of unknown cause. The acute phase is characterized by edema and hyaline membrane formation. The later phase is characterized by airspace and/or interstitial organization (5). The histologic pattern is indistinguishable from that of acute respiratory distress syndrome.

Radiographs and CT scans.—In the acute phase, patchy bilateral ground-glass opacities are seen (6), often with some sparing of individual lobules, producing a geographic appearance; dense opacification is seen in the dependent lung (Fig 1). In the organizing phase, architectural distortion, traction bronchiectasis, cysts, and reticular opacities are seen (7).

Figure 2: Transverse CT scan shows air bronchogram as air-filled bronchi (arrows) against background of high-attenuation lung.

air bronchogram

Radiographs and CT scans.—An air bronchogram is a pattern of air-filled (low-attenuation) bronchi on a background of opaque (high-attenuation) airless lung (Fig 2). The sign implies *(a)* patency of proximal airways and *(b)* evacuation of alveolar air by means of absorption (atelectasis) or replacement (eg, pneumonia) or a combination of these processes. In rare cases, the displacement of air is the result of marked interstitial expansion (eg, lymphoma) (8).
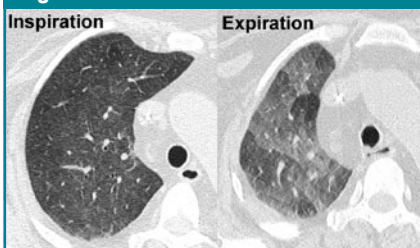
Figure 3

Figure 3: Magnified chest radiograph shows air crescent (arrows) adjacent to mycetoma.

air crescent

Radiographs and CT scans.—An air crescent is a collection of air in a crescentic shape that separates the wall of a cavity from an inner mass (Fig 3). The air crescent sign is often considered characteristic of either *Aspergillus* colonization of preexisting cavities or retraction of infarcted lung in angioinvasive aspergillosis (9,10). However, the air crescent sign has also been reported in other conditions, including tuberculosis, Wegener granulomatosis, intracavitary hemorrhage, and lung cancer. (See also *mycetoma.*)

Figure 4

Figure 4: Transverse CT scans at end inspiration and end expiration show air trapping.

air trapping

*Pathophysiology.*—Air trapping is retention of air in the lung distal to an obstruction (usually partial).

CT scans.—Air trapping is seen on end-expiration CT scans as parenchymal areas with less than normal increase in attenuation and lack of volume reduction. Comparison between inspiratory and expiratory CT scans can be helpful when air trapping is subtle or diffuse (11,12) (Fig 4). Differentiation from areas of decreased attenuation resulting from hypoperfusion as a consequence of an occlusive vascular disorder (eg, chronic thromboembolism) may be problematic (13), but other findings of airways versus vascular disease are usually present. (See also *mosaic attenuation pattern.*)

airspace

Anatomy.—An airspace is the gas-containing part of the lung, including the respiratory bronchioles but excluding purely conducting airways, such as terminal bronchioles.

Radiographs and CT scans.—This term is used in conjunction with *consolidation, opacity,* and *nodules* to designate the filling of airspaces with the products of disease (14).
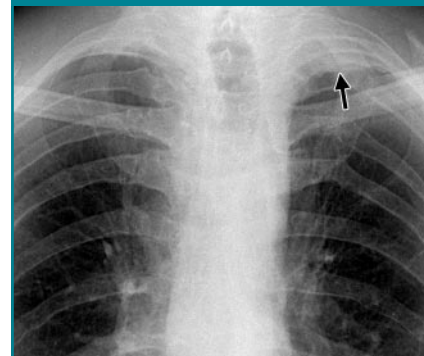
Figure 5
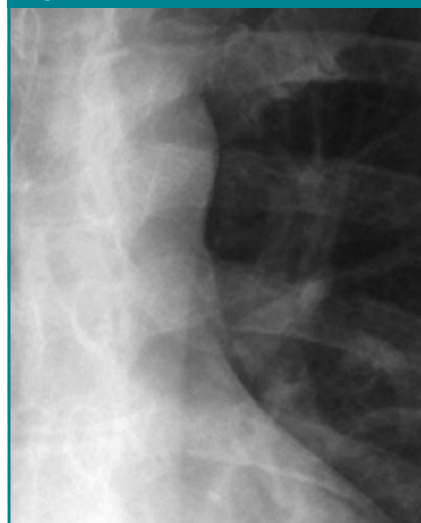
Figure 5: Magnified chest radiograph shows aortopulmonary window.

aortopulmonary window

Anatomy.—The aortopulmonary window is the mediastinal region bounded anteriorly by the ascending aorta, posteriorly by the descending aorta, cranially by the aortic arch, inferiorly by the left pulmonary artery, medially by the ligamentum arteriosum, and laterally by the pleura and left lung (15,16).

Radiographs and CT scans.—Focal concavity in the left mediastinal border below the aorta and above the left pulmonary artery can be seen on a frontal radiograph (Fig 5). Its appearance may be modified by tortuosity of the aorta. The aortopulmonary window is a common site of lymphadenopathy in a variety of inflammatory and neoplastic diseases.

Figure 6

Figure 6: Magnified chest radiograph shows apical cap (arrow).

apical cap

Pathology.—An apical cap is a caplike lesion at the lung apex, usually caused by intrapulmonary and pleural fibrosis pulling down extrapleural fat (17) or possibly by chronic ischemia resulting in hyaline plaque formation on the visceral pleura (18). The prevalence increases with age. It can also be seen in hematoma resulting from aortic rupture or in other fluid collection associated with infection or tumor, either outside the parietal pleura or loculated within the pleural space (19).

Radiographs and CT scans.—The usual appearance is of homogeneous soft-tissue attenuation capping the ex-

treme lung apex (uni- or bilaterally), with a sharp or irregular lower border (Fig 6). Thickness is variable, ranging up to about 30 mm (17). An apical cap occasionally mimics apical consolidation on transverse CT scans.
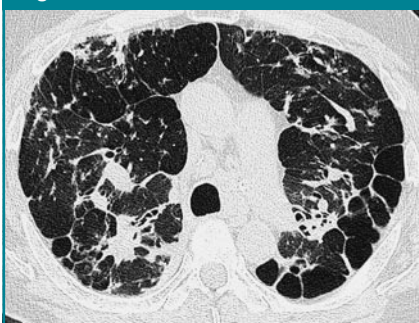
Figure 7: Transverse CT scan shows architectural distortion caused by pulmonary fibrosis.

architectural distortion

Pathology.—Architectural distortion is characterized by abnormal displacement of bronchi, vessels, fissures, or septa caused by diffuse or localized lung disease, particularly interstitial fibrosis.

CT scans.—Lung anatomy has a distorted appearance and is usually associated with pulmonary fibrosis (Fig 7) and accompanied by volume loss.


Figure 8: Transverse CT scan shows atelectasis of right middle lobe as increased attenuation (arrows) adjacent to right border of heart.

atelectasis

Pathophysiology.—Atelectasis is reduced inflation of all or part of the lung (20). One of the commonest mechanisms is resorption of air distal to airway obstruction (eg, an endobronchial neoplasm) (21). The synonym *collapse* is often used interchangeably with *atelectasis,* particularly when it is severe or accompanied by obvious increase in lung opacity.

Radiographs and CT scans.—Reduced volume is seen, accompanied by increased opacity (chest radiograph) or attenuation (CT scan) in the affected part of the lung (Fig 8). Atelectasis is often associated with abnormal displacement of fissures, bronchi, vessels, diaphragm, heart, or mediastinum (22). The distribution can be lobar, segmental, or subsegmental. Atelectasis is often qualified by descriptors such as *linear, discoid,* or *platelike.* (See also *linear atelectasis, rounded atelectasis.*)
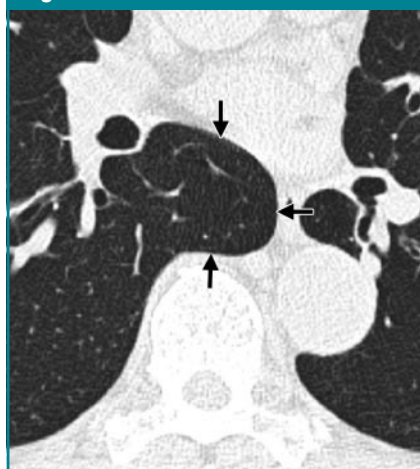
Figure 9: Transverse CT scan shows azygoesophageal recess (arrows).

azygoesophageal recess

Anatomy.—The azygoesophageal recess is a right posterior mediastinal recess into which the edge of the right lower lobe extends. It is limited superiorly by the azygos arch, posteriorly by the azygos vein and pleura anterior to the vertebral column, and medially by the esophagus and adjacent structures.

Radiographs and CT scans.—On a frontal chest radiograph, the recess is seen as a vertically oriented interface between the right lower lobe and the adjacent mediastinum (the medial limit of the recess). Superiorly, the interface is seen as a smooth arc with convexity to the left. Disappearance or distortion of part of the interface suggests disease (eg, subcarinal lymphadenopathy). On CT scans, the recess (Fig 9) merits attention because small lesions located in the recess will often be invisible on chest radiographs (23).

azygos fissure

See *fissure.*
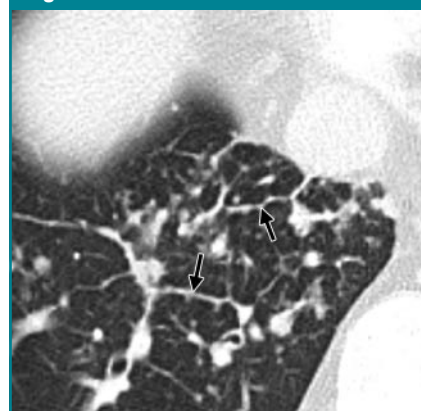
Figure 10: Transverse CT scan shows beaded septum sign (arrows).

beaded septum sign

CT scans.—This sign consists of irregular and nodular thickening of interlobular septa reminiscent of a row of beads (Fig 10). It is frequently seen in lymphangitic spread of cancer and less often in sarcoidosis (24).

bleb

Anatomy.—A bleb is a small gas-containing space within the visceral pleura or in the subpleural lung, not larger than 1 cm in diameter (25).

CT scans.—A bleb appears as a thin-walled cystic air space contiguous with the pleura. Because the arbitrary (size) distinction between a bleb and

bulla is of little clinical importance, the use of this term by radiologists is discouraged.
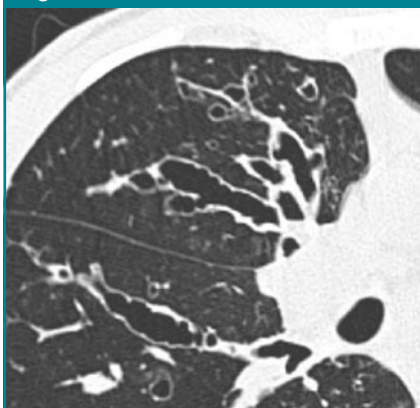
Figure 11: Transverse CT scan shows varicose bronchiectasis.

bronchiectasis

Pathology.—Bronchiectasis is irreversible localized or diffuse bronchial dilatation, usually resulting from chronic infection, proximal airway obstruction, or congenital bronchial abnormality (26). (See also *traction bronchiectasis.*)

Radiographs and CT scans.—Morphologic criteria on thin-section CT scans include bronchial dilatation with respect to the accompanying pulmonary artery (signet ring sign), lack of tapering of bronchi, and identification of bronchi within 1 cm of the pleural surface (27) (Fig 11). Bronchiectasis may be classified as cylindric, varicose, or cystic, depending on the appearance of the affected bronchi. It is often accompanied by bronchial wall thickening, mucoid impaction, and small-airways abnormalities (27–29). (See also *signet ring sign.*)

bronchiole

Anatomy.—Bronchioles are non–cartilage-containing airways. Terminal bronchioles are the most distal of the purely conducting airways; they give rise to respiratory bronchioles, from which the alveoli arise and permit gas exchange. Respiratory bronchioles branch into multiple alveolar ducts (30).

Radiographs and CT scans.—Bronchioles are not identifiable in healthy individuals, because the bronchiolar walls are too thin (4). In inflammatory small-airways disease, however, thickened or plugged bronchioles may be seen as a nodular pattern on a chest radiograph or as a tree-in-bud pattern on CT scans.

Figure 12: Transverse CT scan shows bronchiolectasis within fibrotic lung (arrow).

bronchiolectasis

Pathology.—Bronchiolectasis is defined as dilatation of bronchioles. It is caused by inflammatory airways disease (potentially reversible) or, more frequently, fibrosis.

CT scans.—When dilated bronchioles are filled with exudate and are thick walled, they are visible as a tree-in-bud pattern or as centrilobular nodules (31,32). In traction bronchiolectasis, the dilated bronchioles are seen as small, cystic, tubular airspaces, associated with CT findings of fibrosis (Fig 12). (See also *traction bronchiectasis and traction bronchiolectasis, tree-in-bud pattern.*)
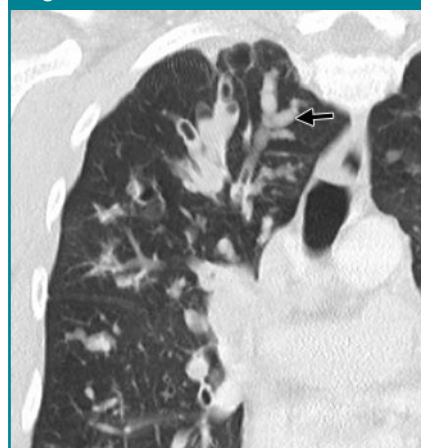
bronchiolitis

Pathology.—Bronchiolitis is bronchiolar inflammation of various causes (33).

CT scans.—This direct sign of bronchiolar inflammation (eg, infectious cause) is most often seen as the tree-in-bud pattern, centrilobular nodules, and bronchiolar wall thickening on CT scans. (See also *small-airways disease, tree-in-bud pattern.*)

Figure 13: Coronal CT scan shows bronchocele (arrow).

bronchocele

Pathology.—A bronchocele is bronchial dilatation due to retained secretions (mucoid impaction) usually caused by proximal obstruction, either congenital (eg, bronchial atresia) or acquired (eg, obstructing cancer) (34).

Radiographs and CT scans.—A bronchocele is a tubular or branching Y- or V-shaped structure that may resemble a gloved finger (Fig 13). The CT attenuation of the mucus is generally that of soft tissue but may be modified by its composition (eg, high-attenuation material in allergic bronchopulmonary aspergillosis). In the case of bronchial atresia, the surrounding lung may be of decreased attenuation because of reduced ventilation and, thus, perfusion.

hinhanhykhoa.com
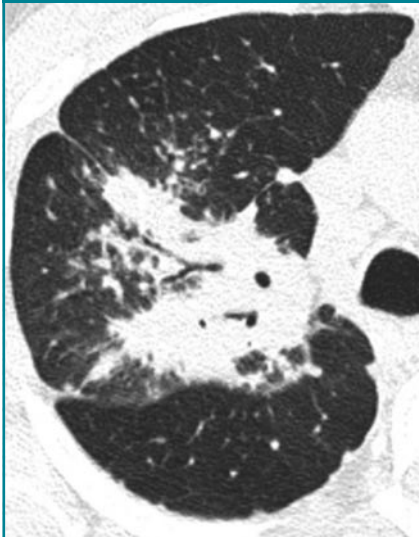
Figure 14: Transverse CT scan shows consolidation with bronchocentric distribution.

bronchocentric

CT scans.—This descriptor is applied to disease that is conspicuously centered on macroscopic bronchovascular bundles (Fig 14). Examples of diseases with a bronchocentric distribution include sarcoidosis (35), Kaposi sarcoma (36), and organizing pneumonia (37).


Figure 15: Transverse CT scan shows a broncholith (arrows).

broncholith

Pathology.—A broncholith, a calcified peribronchial lymph node that erodes into an adjacent bronchus, is most often the consequence of *Histoplasma* or tuberculous infection.

Radiographs and CT scans.—The imaging appearance is of a small calcific focus in or immediately adjacent to an airway (Fig 15), most frequently the right middle lobe bronchus. Broncholiths are readily identified on CT scans (38). Distal obstructive changes may include atelectasis, mucoid impaction, and bronchiectasis.
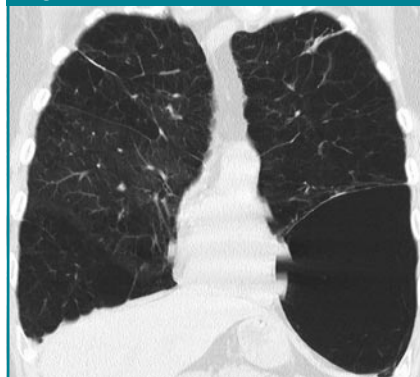
**Figure 16:** Coronal CT scan shows large bulla in left lower lung zone.

bulla

Pathology.—An airspace measuring more than 1 cm—usually several centimeters—in diameter, sharply demarcated by a thin wall that is no greater than 1 mm in thickness. A bulla is usually accompanied by emphysematous changes in the adjacent lung. (See also *bullous emphysema.*)

Radiographs and CT scans.—A bulla appears as a rounded focal lucency or area of decreased attenuation, 1 cm or more in diameter, bounded by a thin wall (Fig 16). Multiple bullae are often present and are associated with other signs of pulmonary emphysema (centrilobular and paraseptal).

bullous emphysema

Pathology.—Bullous emphysema is bullous destruction of the lung parenchyma, usually on a background of paraseptal or panacinar emphysema. (See also *emphysema, bulla.*)
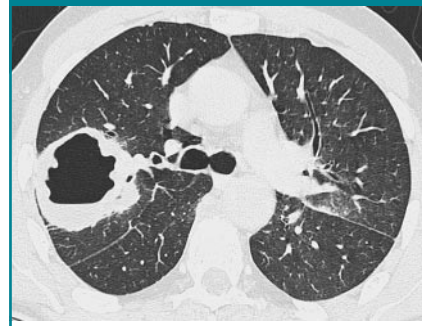
Figure 17: Transverse CT scan shows cavitating mass in right upper lobe.

cavity

Radiographs and CT scans.—A cavity is a gas-filled space, seen as a lucency or low-attenuation area, within pulmonary consolidation, a mass, or a nodule (Fig 17). In the case of cavitating consolidation, the original consolidation may resolve and leave only a thin wall. A cavity is usually produced by the expulsion or drainage of a necrotic part of the lesion via the bronchial tree. It sometimes contains a fluid level. *Cavity* is not a synonym for *abscess.*

centrilobular

Anatomy.—Centrilobular describes the region of the bronchiolovascular core of a secondary pulmonary lobule (4,39,40). This term is also used by pathologists to describe the location of lesions beyond the terminal bronchiole that center on respiratory bronchioles or even alveolar ducts.

CT scans.–A small dotlike or linear opacity in the center of a normal secondary pulmonary lobule, most obvious within 1 cm of a pleural surface, represents the intralobular artery (approximately 1 mm in diameter) (41). Centrilobular abnormalities include *(a)* nodules, *(b)* a tree-in-bud pattern indicating small-airways disease, *(c)* increased vis-

Radiology

ibility of centrilobular structures due to thickening or infiltration of the adjacent interstitium, or *(d)* abnormal areas of low attenuation caused by centrilobular emphysema (4). (See also *lobular core structures.*)

Figure 18

Figure 18: Transverse CT scan shows centrilobular emphysema.

centrilobular emphysema

Pathology.—Centrilobular emphysema is characterized by destroyed centrilobular alveolar walls and enlargement of respiratory bronchioles and associated alveoli (42,43). This is the commonest form of emphysema in cigarette smokers.

CT scans.—CT findings are centrilobular areas of decreased attenuation, usually without visible walls, of nonuniform distribution and predominantly located in upper lung zones (44) (Fig 18). The term *centriacinar emphysema* is synonymous. (See also *emphysema.*)

collapse

See *atelectasis.*

Figure 19

Figure 19: Transverse CT scan shows multifocal consolidation.

consolidation

Pathology.—Consolidation refers to an exudate or other product of disease that replaces alveolar air, rendering the lung solid (as in infective pneumonia).

Radiographs and CT scans.—Consolidation appears as a homogeneous increase in pulmonary parenchymal attenuation that obscures the margins of vessels and airway walls (45) (Fig 19). An air bronchogram may be present. The attenuation characteristics of consolidated lung are only rarely helpful in differential diagnosis (eg, decreased attenuation in lipoid pneumonia [46] and increased in amiodarone toxicity [47]).

Figure 20

Figure 20: Transverse CT scan shows crazy-paving pattern.

crazy-paving pattern

CT scans.—This pattern appears as thickened interlobular septa and intralobular lines superimposed on a background of ground-glass opacity (Fig 20), resembling irregularly shaped paving stones. The crazy-paving pattern is often sharply demarcated from more normal lung and may have a geographic outline. It was originally reported in patients with alveolar proteinosis (48) and is also encountered in other diffuse lung diseases (49) that affect both the interstitial and airspace compartments, such as lipoid pneumonia (50).

cryptogenic organizing pneumonia, or COP

See *organizing pneumonia.*

Figure 21

Figure 21: Coronal CT scan shows a cyst.

cyst

Pathology.—A cyst is any round circumscribed space that is surrounded by an epithelial or fibrous wall of variable thickness (51).

Radiographs and CT scans.—A cyst appears as a round parenchymal lucency or low-attenuating area with a well-defined interface with normal lung. Cysts have variable wall thickness but are usually thin-walled (<2 mm) and occur without associated pulmonary emphysema (Fig 21). Cysts in the lung usually contain air but occasionally contain fluid or solid material. The term is often used to describe enlarged thin-walled airspaces in patients with lymphangioleiomyomatosis (52) or Langerhans cell histiocytosis (53); thicker-walled honeycomb cysts are seen in patients with end-stage fibrosis (54). (See also *bleb, bulla, honeycombing, pneumatocele.*)

Figure 22

Figure 22: Transverse CT scan in a patient with desquamative interstitial pneumonia.

desquamative interstitial pneumonia, or DIP

Pathology.—Histologically, DIP is characterized by the widespread accumulation of an excess of macrophages in the distal airspaces. The macrophages are uniformly distributed, unlike in respiratory bronchiolitis–interstitial lung disease, in which the disease is conspicuously bronchiolocentric. Interstitial involvement is minimal. Most cases of DIP are related to cigarette smoking, but a few are idiopathic or associated with rare inborn errors of metabolism (5).

Radiographs and CT scans.—Ground-glass opacity is the dominant abnormality and tends to have a basal and peripheral distribution (Fig 22). Microcystic or honeycomb changes in the area of ground-glass opacity are seen in some cases (55).

diffuse alveolar damage, or DAD

See *acute interstitial pneumonia.*

emphysema

Pathology.—Emphysema is characterized by permanently enlarged airspaces distal to the terminal bronchiole with destruction of alveolar walls (42,43). Absence of "obvious fibrosis" was historically regarded as an additional criterion (42), but the validity of that criterion has been questioned because some interstitial fibrosis may be present in emphysema secondary to cigarette smoking (56,57). Emphysema is usually classified in terms of the part of the acinus predominantly affected: proximal (centriacinar, more commonly termed *centrilobular,* emphysema), dis-

tal (paraseptal emphysema), or whole acinus (panacinar or, less commonly, panlobular emphysema).

CT scans.—The CT appearance of emphysema consists of focal areas or regions of low attenuation, usually without visible walls (58). In the case of panacinar emphysema, decreased attenuation is more diffuse. (See also *bullous emphysema, centrilobular emphysema, panacinar emphysema, paraseptal emphysema.*)

fissure

Anatomy.—A fissure is the infolding of visceral pleura that separates one lobe or part of a lobe from another; thus, the interlobar fissures are produced by two layers of visceral pleura. Supernumerary fissures usually separate segments rather than lobes. The azygos fissure, unlike the other fissures, is formed by two layers each of visceral and parietal pleura. All fissures (apart from the azygos fissure) may be incomplete.

Radiographs and CT scans.—Fissures appear as linear opacities, normally 1 mm or less in thickness, that correspond in position and extent to the anatomic fissural separation of pulmonary lobes or segments. Qualifiers include minor, major, horizontal, oblique, accessory, anomalous, azygos, and inferior accessory.

folded lung

See *rounded atelectasis.*

fungus ball

See *mycetoma.*

gas trapping

See *air trapping.*

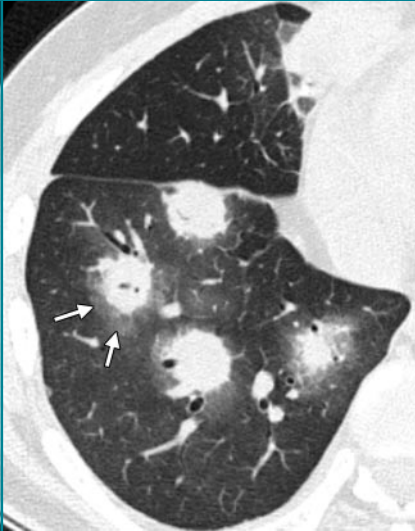#### ground-glass nodule

See *nodule.*

Figure 23

Figure 23: Transverse CT scan shows ground-glass opacity.

ground-glass opacity

Radiographs and CT scans.—On chest radiographs, ground-glass opacity appears as an area of hazy increased lung opacity, usually extensive, within which margins of pulmonary vessels may be indistinct. On CT scans, it appears as hazy increased opacity of lung, with preservation of bronchial and vascular margins (Fig 23). It is caused by partial filling of airspaces, interstitial thickening (due to fluid, cells, and/or fibrosis), partial collapse of alveoli, increased capillary blood volume, or a combination of these, the common factor being the partial displacement of air (59,60). Ground-glass opacity is less opaque than consolidation, in which bronchovascular margins are obscured. (See also *consolidation.*)

Figure 24: Transverse CT scan shows several nodules exhibiting the halo sign (arrows).

Figure 25: Transverse CT scan shows honeycombing.

Figure 26: Coronal CT scan shows reticular opacities and honeycombing in the lower zones, typical of idiopathic pulmonary fibrosis.
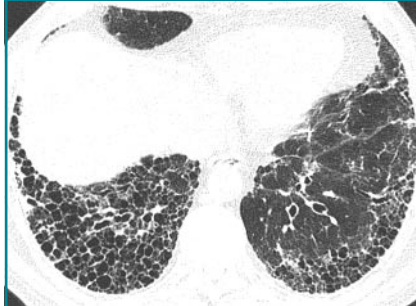
halo sign

CT scans.—The halo sign is a CT finding of ground-glass opacity surrounding a nodule or mass (Fig 24). It was first described as a sign of hemorrhage around foci of invasive aspergillosis (61). The halo sign is nonspecific and may also be caused by hemorrhage associated with other types of nodules (62) or by local pulmonary infiltration by neoplasm (eg, adenocarcinoma). (See also *reversed halo sign*.)

hilum

Anatomy.—*Hilum* is a generic term that describes the indentation in the surface of an organ, where vessels and nerves connect with the organ. It is the site on the medial aspect of the lung where the vessels and bronchi enter and leave the lung.

Radiographs and CT scans.—A hilum appears as a composite opacity at the root of each lung produced by bronchi, arteries, veins, lymph nodes, nerves, and other tissue. The terms *hilum* (singular) and *hila* (plural) are preferred to *hilus* and *hili* respectively; the adjectival form is *hilar*.

honeycombing
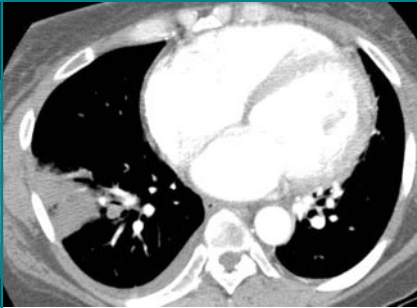
Pathology.—Honeycombing represents destroyed and fibrotic lung tissue containing numerous cystic airspaces with thick fibrous walls, representing the late stage of various lung diseases, with complete loss of acinar architecture. The cysts range in size from a few millimeters to several centimeters in diameter, have variable wall thickness, and are lined by metaplastic bronchiolar epithelium (51).

Radiographs and CT scans.—On chest radiographs, honeycombing appears as closely approximated ring shadows, typically 3–10 mm in diameter with walls 1–3 mm in thickness, that resemble a honeycomb; the finding implies end-stage lung disease. On CT scans, the appearance is of clustered cystic air spaces, typically of comparable diameters on the order of 3–10 mm but occasionally as large as 2.5 cm (Fig 25). Honeycombing is usually subpleural and is characterized by well-defined walls (54). It is a CT feature of established pulmonary fibrosis (5). Because honeycombing is often considered specific for pulmonary fibrosis and is an important criterion in the diagnosis of usual interstitial pneumonia (63), the term should be used with care, as it may directly impact patient care.
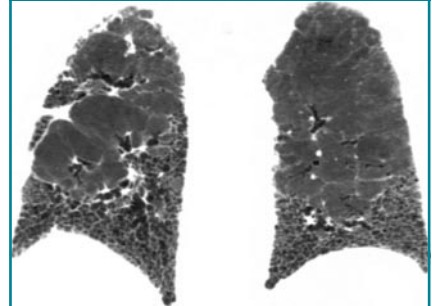
idiopathic pulmonary fibrosis

Pathology.—Idiopathic pulmonary fibrosis is a specific form of chronic fibrosing interstitial pneumonia of unknown cause and is characterized by a histologic pattern of usual interstitial pneumonia (5,64).

Radiographs and CT scans.—The typical imaging findings are reticular opacities and honeycombing, with a predominantly peripheral and basal distribution (Fig 26). Ground-glass opacity, if present, is less extensive than reticular and honeycombing patterns. The typical radiologic findings (65,66) are also encountered in usual interstitial pneumonia secondary to specific causes, such as asbestos-induced pulmonary fibrosis (asbestosis), and the diagnosis is usually one of exclusion. (See also *usual interstitial pneumonia*.)

Figure 27

Figure 27: Transverse CT scan shows pulmonary infarction.

Figure 28

Figure 28: Transverse CT scan shows interlobular septal thickening and pleural effusions.

Figure 29

Figure 29: Transverse CT scan shows interlobular septum (arrow) in a healthy individual.

infarction
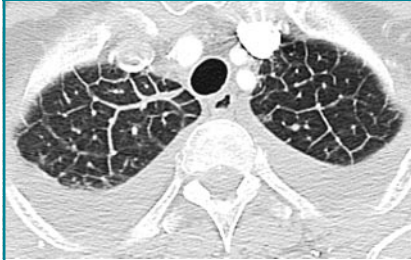
Pathology.—Infarction is a process that may result in ischemic necrosis, usually the consequence of vascular compromise such as occlusion of a feeding pulmonary artery by an embolus (venous infarction is rare but recognized). Necrosis is relatively uncommon because tissue viability is maintained by the bronchial arterial blood supply. Pulmonary infarction may be secondary to a vasculitis (eg, Wegener granulomatosis).

Radiographs and CT scans.—A pulmonary infarct is typically triangular or dome-shaped, with the base abutting the pleura and the apex directed toward the hilum (Fig 27). The opacity represents local hemorrhage with or without central tissue necrosis (67,68).

infiltrate

Radiographs and CT scans.—Formerly used as a term to describe a region of pulmonary opacification caused by airspace or interstitial disease seen on radiographs and CT scans. *Infiltrate* remains controversial because it means different things to different people (69). The term is no longer recommended, and has been largely replaced by other descriptors. The term *opacity,* with relevant qualifiers, is preferred.
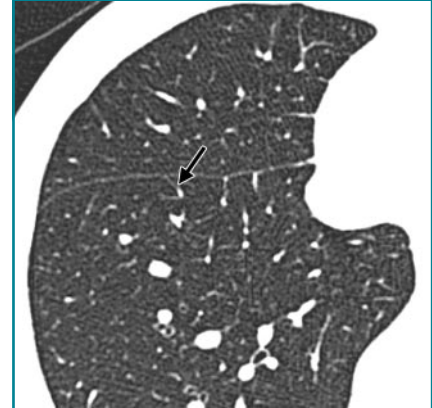
interlobular septal thickening

Radiographs and CT scans.—This finding is seen on chest radiographs as thin linear opacities at right angles to and in contact with the lateral pleural surfaces near the lung bases (Kerley B lines); it is seen most frequently in lymphangitic spread of cancer or pulmonary edema. Kerley A lines are predominantly situated in the upper lobes, are 2–6 cm long, and can be seen as fine lines radially oriented toward the hila. In recent years, the anatomically descriptive terms *septal lines* and *septal thickening* have gained favor over *Kerley lines.* On CT scans, disease affecting one of the components of the septa (see *interlobular septum*) may be responsible for thickening and so render septa visible. On thin-section CT scans, septal thickening may be smooth or nodular (70) (Fig 28), which may help refine the differential diagnosis. (See also *interlobular septum, beaded septum.*)

interlobular septum

Anatomy.—Interlobular septa are sheet-like structures 10–20-mm long that form the borders of lobules; they are more or less perpendicular to the pleura in the periphery. Interlobular septa are composed of connective tissue and contain lymphatic vessels and pulmonary venules.

Radiographs and CT scans.—Interlobular septa appear as thin linear opacities between lobules (Fig 29); these septa are to be distinguished from centrilobular structures. They are not usually seen in the healthy lung (normal septa are approximately 0.1 mm thick) but are clearly visible when thickened (eg, by pulmonary edema). (See also *interlobular septal thickening, lobule.*)
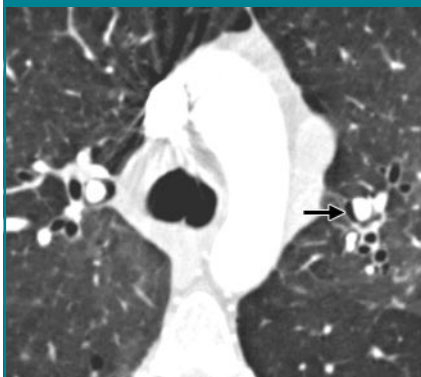
Figure 30: Transverse CT scan shows interstitial emphysema (arrow).

interstitial emphysema

Pathology.—Interstitial emphysema is characterized by air dissecting within the interstitium of the lung, typically in the peribronchovascular sheaths, interlobular septa, and visceral pleura. It is most commonly seen in neonates receiving mechanical ventilation.

   Radiographs and CT scans.—Interstitial emphysema is rarely recognized radiographically in adults and is infrequently seen on CT scans (Fig 30). It appears as perivascular lucent or lowattenuating halos and small cysts (71,72).

interstitium

Anatomy.—The interstitium consists of a continuum of connective tissue throughout the lung comprising three subdivisions: *(a)* the bronchovascular (axial) interstitium, surrounding and supporting the bronchi, arteries, and veins from the hilum to the level of the respiratory bronchiole; *(b)* the parenchymal (acinar) interstitium, situated between alveolar and capillary basement membranes; and *(c)* the subpleural connective tissue contiguous with the interlobular septa (73).
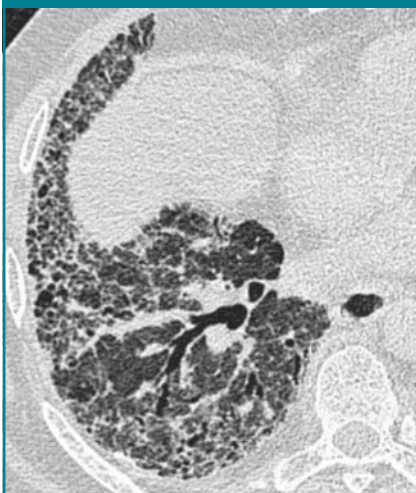
Figure 31: Transverse CT scan shows Intralobular lines.

intralobular lines

CT scans.—Intralobular lines are visible as fine linear opacities in a lobule when the intralobular interstitial tissue is abnormally thickened (Fig 31). When numerous, they may appear as a fine reticular pattern. Intralobular lines may be seen in various conditions, including interstitial fibrosis and alveolar proteinosis (41).

Figure 32: Chest radiograph shows juxtaphrenic peak of the right hemidiaphragm.

juxtaphrenic peak

Radiographs and CT scans.—A juxtaphrenic peak is a small triangular opacity based at the apex of the dome of a hemidiaphragm, associated with upper lobe volume loss of any cause (eg, postirradiation fibrosis or upper lobectomy) (74). It is most readily appreciated on a frontal chest radiograph (Fig 32). The peak is caused by upward retraction of the inferior accessory fissure (75) or an intrapulmonary septum associated with the pulmonary ligament (76).

Figure 33: Chest radiograph shows basal linear atelectasis.

linear atelectasis

Radiographs and CT scans.—Linear atelectasis is a focal area of subsegmental atelectasis with a linear configuration, almost always extending to the pleura (74). It is commonly horizontal but sometimes oblique or vertical. The thickness of the atelectasis may range from a few millimeters to more than 1 cm (Fig 33). Linear atelectasis is also referred to as *discoid* or *platelike atelectasis*. (See also *atelectasis*.)

lobe

Anatomy.—The lobe is the principal division of the lungs (normally, three lobes on the right and two on the left); each lobe is enveloped by visceral pleura, except at the lung root (hilum) and when an interlobar fissure is incomplete.

Figure 34: Transverse CT scan shows lobular core structure (arrow).

lobular core structures

Anatomy.—Lobular core structures are the central structures in secondary pulmonary lobules and consist of a centrilobular artery and bronchiole (40).

CT scans.—The pulmonary artery and its immediate branches are visible in the center of a secondary lobule on thin-section CT scans, particularly if thickened (eg, by pulmonary edema) (Fig 34). These arteries measure approximately 0.5–1.0 mm in diameter. However, the normal bronchiole in the center of the secondary pulmonary lobule cannot be seen on thin-section CT scans because of the thinness of its wall (approximately 0.15 mm) (4,41). (See also *centrilobular, lobule.*)
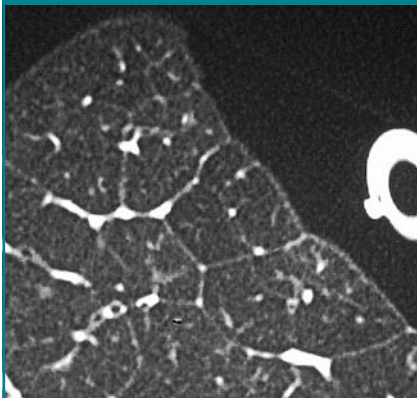
Figure 35: CT scan of resected lung shows lobules.

lobule

Anatomy.—The lobule is the smallest unit of lung surrounded by connective-tissue septa, as defined by Miller (78) and Heitzman et al (40). The lobule is also referred to as the *secondary pulmonary lobule;* it contains a variable number of acini, is irregularly polyhedral in shape, and varies in size from 1.0 to 2.5 cm in diameter. The centrilobular structures, or core structures, include bronchioles and their accompanying pulmonary arterioles and lymphatic vessels. The connective-tissue septa surrounding the pulmonary lobule—the interlobular septa, which contain veins and lymphatic vessels—are best developed in the periphery in the anterior, lateral, and juxtamediastinal regions of the upper and middle lobes.

CT scans.—On thin-section CT scans, the three basic components of the lobule—the interlobular septa and septal structures, the central lobular region (centrilobular structures), and the lobular parenchyma— can be identified, particularly in disease states. Peripheral lobules are more uniform in appearance and pyramidal in shape than are central lobules (4) (Fig 35). (See also *interlobular septa, lobular core structures.*)
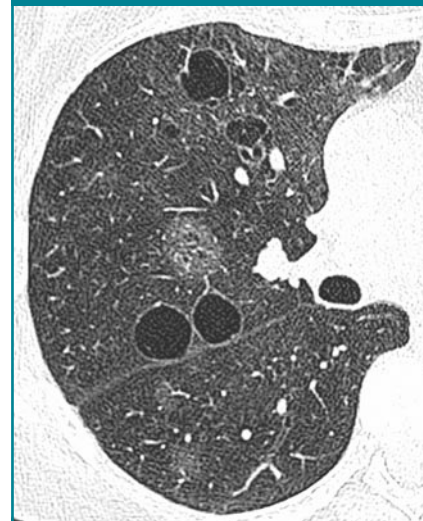

Figure 36: Transverse CT scan shows lymphadenopathy (enlarged mediastinal lymph nodes).

lymphadenopathy

Pathology.—By common usage, the term *lymphadenopathy* is usually restricted to enlargement, due to any cause, of the lymph nodes. Synonyms include *lymph node enlargement* (preferred) and *adenopathy.*

CT scans.—There is a wide range in the size of normal lymph nodes. Mediastinal and hilar lymph nodes range in size from sub-CT resolution to 12 mm. Somewhat arbitrary thresholds for the upper limit of normal of 1 cm in short-axis diameter for mediastinal nodes (79) and 3 mm for most hilar nodes (80) have been reported, but size criteria do not allow reliable differentiation between healthy and diseased lymph nodes (Fig 36).

Figure 37: Transverse CT scan shows ground-glass opacities and perivascular cysts in a patient with lymphoid interstitial pneumonia.

lymphoid interstitial pneumonia, or LIP

Pathology.—LIP is a rare disease characterized by diffuse pulmonary lymphoid proliferation with predominant interstitial involvement. It is included in the spectrum of interstitial pneumonias and is distinct from diffuse lymphomas of the lung. Features include diffuse hyperplasia of bronchus-associated lymphoid tissue and diffuse polyclonal lym-

phoid cell infiltrates surrounding the airways and expanding the lung interstitium. LIP is usually associated with autoimmune diseases or human immunodeficiency virus infection (5,81).

CT scans.—Ground-glass opacity is the dominant abnormality, and thin-walled perivascular cysts may be present (Fig 37). Lung nodules, a reticular pattern, interlobular septal and bronchovascular thickening, and widespread consolidation may also occur (82,83).

mass

Radiographs and CT scans.—A mass is any pulmonary, pleural, or mediastinal lesion seen on chest radiographs as an opacity greater than 3 cm in diameter (without regard to contour, border, or density characteristics). *Mass* usually implies a solid or partly solid opacity. CT allows more exact evaluation of size, location, attenuation, and other features. (See also *nodule.*)

mediastinal compartments

Anatomy.—Nominal anatomic compartments of the mediastinum include the anterior, middle, posterior, and (in some schemes) superior compartments. The anterior compartment is bounded anteriorly by the sternum and posteriorly by the anterior surface of the pericardium, the ascending aorta, and the brachiocephalic vessels. The middle compartment is bounded by the posterior margin of the anterior division and the anterior margin of the posterior division. The posterior compartment is bounded anteriorly by the posterior margins of the pericardium and great vessels and posteriorly by the thoracic vertebral bodies. In the four-compartment model, the superior compartment is defined as the compartment above the plane between the sternal angle to the T4-5 intervertebral disk or, more simply, above the aortic arch (84,85). Exact anatomic boundaries between the compartments do not exist, and there are no barriers (other than the pericardium) to prevent the spread of disease between compartments. Other classifications exist, but the three- and four-

compartment models are the most commonly used.

micronodule

CT scans.—A micronodule is a discrete, small, round, focal opacity. A variety of diameters have been used in the past to define a micronodule; for example, a diameter of no greater than 7 mm (86). Use of the term is most often limited to nodules with a diameter of less than 5 mm (87) or less than 3 mm (88). It is recommended that the term be reserved for opacities less than 3 mm in diameter. (See also *nodule, miliary pattern.*)

Figure 38: Magnified chest radiograph shows miliary pattern.

miliary pattern

Radiographs and CT scans.—On chest radiographs, the miliary pattern consists of profuse tiny, discrete, rounded pulmonary opacities (≤3 mm in diameter) that are generally uniform in size and diffusely distributed throughout the lungs (Fig 38). This pattern is a manifestation of hematogenous spread of tuberculosis and metastatic disease. Thin-section CT scans show widespread, randomly distributed micronodules.

Figure 39: Transverse CT scan shows mosaic attenuation pattern caused by obliterative small-airways disease.

mosaic attenuation pattern

CT scans.—This pattern appears as patchwork of regions of differing attenuation that may represent *(a)* patchy interstitial disease, *(b)* obliterative small-airways disease (Fig 39), or *(c)* occlusive vascular disease (89). *Mosaic attenuation pattern* is a more inclusive term than the original terms *mosaic oligemia* and *perfusion* (90). Air trapping secondary to bronchial or bronchiolar obstruction may produce focal zones of decreased attenuation, an appearance that can be enhanced by using expiratory CT (91,92). The mosaic attenuation pattern can also be produced by interstitial lung disease characterized by ground-glass opacity; in this situation, areas of higher attenuation represent the interstitial process and areas of lower attenuation represent the normal lung.

mosaic oligemia, perfusion

See *mosaic attenuation pattern.*

Figure 40
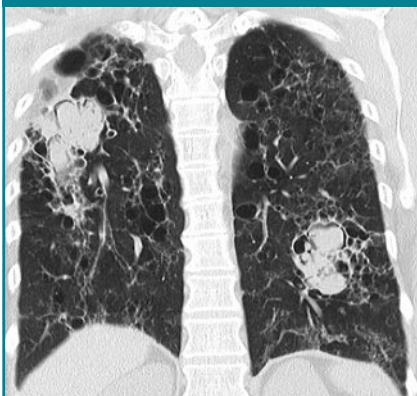
Figure 40: Coronal CT scan shows mycetomas in both lungs.

mycetoma

Pathology.—A mycetoma is a discrete mass of intertwined hyphae, usually of an *Aspergillus* species, matted together by mucus, fibrin, and cellular debris colonizing a cavity, usually from prior fibrocavitary disease (eg, tuberculosis or sarcoidosis).

Radiographs and CT scans.—A mycetoma may move to a dependent location when the patient changes position and may show an air crescent sign (Fig 40). CT scans may show a spongelike pattern and foci of calcification in the mycetoma (93). A synonym is *fungus ball.* (See also *air crescent.*)

Figure 41

Figure 41: Magnified chest radiograph shows a nodular pattern.

nodular pattern

Radiographs and CT scans.—A nodular pattern is characterized on chest radiographs by the presence of innumerable small rounded opacities that are discrete and range in diameter from 2 to 10 mm (Fig 41). The distribution is widespread but not necessarily uniform. On CT scans, the pattern may be classified as one of three anatomic distributions: centrilobular, lymphatic, or random. (See also *nodule.*)
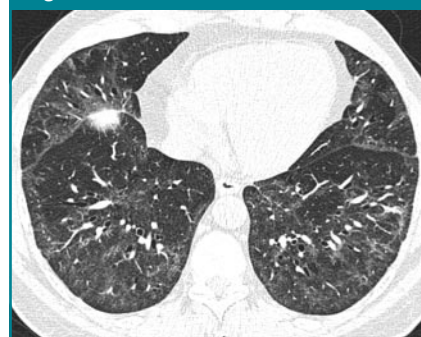
Figure 42

Figure 42: Transverse CT scan shows irregular nodule in left lower lobe.

nodule

Radiographs and CT scans.—The chest radiographic appearance of a nodule is a rounded opacity, well or poorly defined, measuring up to 3 cm in diameter. *(a)* Acinar nodules are round or ovoid poorly defined pulmonary opacities approximately 5–8 mm in diameter, presumed to represent an anatomic acinus rendered opaque by consolidation. This classification is used only in the presence of numerous such opacities. *(b)* A pseudonodule mimics a pulmonary nodule; it represents, for example, a rib fracture, a skin lesion, a device on the surface of the patient, anatomic variants, or composite areas of increased opacity (94).

On CT scans, a nodule appears as a rounded or irregular opacity, well or poorly defined, measuring up to 3 cm in diameter (Fig 42). *(a)* Centrilobular nodules appear separated by several millimeters from the pleural surfaces, fissures, and interlobular septa. They may be of soft-tissue or ground-glass attenuation. Ranging in size from a few millimeters to a centimeter, centrilobular nodules are usually ill-defined (4). *(b)* A micronodule is less than 3 mm in diameter (see also *micronodule*). *(c)* A ground-glass nodule (synonym, *nonsolid nodule*) manifests as hazy increased attenuation in the lung that does not obliterate the bronchial and vascular margins. *(d)* A solid nodule has homogenous soft-tissue attenuation. *(e)* A part-solid nodule (synonym, *semisolid nodule*) consists of both ground-glass and solid soft-tissue attenuation components. (See also *mass.*)

Figure 43

Figure 43: Transverse CT scan shows nonspecific interstitial pneumonia.

nonspecific interstitial pneumonia, or NSIP

Pathology.—NSIP is characterized by a histologic pattern of uniform interstitial involvement by varying degrees of chronic inflammation or fibrosis. NSIP may be idiopathic or seen in other settings, including collagen vascular disease, hypersensitivity pneumonitis, drug-induced lung disease, infection, and immunodeficiency (including human immunodeficiency virus infection) (5).

CT scans.—NSIP has variable thin-

section CT appearances: The most frequent is ground-glass opacities with reticulation, traction bronchiectasis or bronchiolectasis, and little or no honeycombing (Fig 43). The distribution is usually basal and subpleural (95).
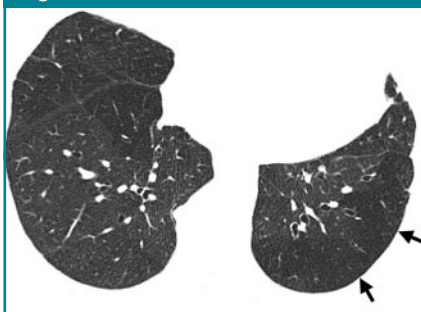
Figure 44

Figure 44: Transverse CT scan shows oligemia (arrows) in left lung.

oligemia

Pathophysiology.—Oligemia is a reduction in pulmonary blood volume. Most frequently, this reduction is regional, but occasionally it is generalized. Regional oligemia is usually associated with reduced blood flow in the oligemic area.

Radiographs and CT scans.—Oligemia appears as a regional or widespread decrease in the size and number of identifiable pulmonary vessels (Fig 44), which is indicative of less than normal blood flow. (See also *mosaic attenuation pattern, pulmonary blood flow redistribution.*)

opacity

Radiographs and CT scans.—Opacity refers to any area that preferentially attenuates the x-ray beam and therefore appears more opaque than the surrounding area. It is a nonspecific term that does not indicate the size or pathologic nature of the abnormality. (See also *parenchymal opacification, ground-glass opacity.*)

Figure 45

Figure 45: Transverse CT scan shows cryptogenic organizing pneumonia with subpleural and basal distribution.

organizing pneumonia

Pathology.—Organizing pneumonia manifests as a histologic pattern characterized by loose plugs of connective tissue in the airspaces and distal airways. Interstitial inflammation and fibrosis are minimal or absent. Cryptogenic organizing pneumonia, or COP, is a distinctive clinical disorder among the idiopathic interstitial pneumonias (5), but the histologic pattern of organizing pneumonia is encountered in many different situations, including pulmonary infection, hypersensitivity pneumonitis, and collagen vascular diseases.

Radiographs and CT scans.—Airspace consolidation is the cardinal feature of organizing pneumonia on chest radiographs and CT scans. In COP, the distribution is typically subpleural and basal (Fig 45) and sometimes bronchocentric (96). Other manifestations of organizing pneumonia include ground-glass opacity, tree-in-bud pattern, and nodular opacities (37).
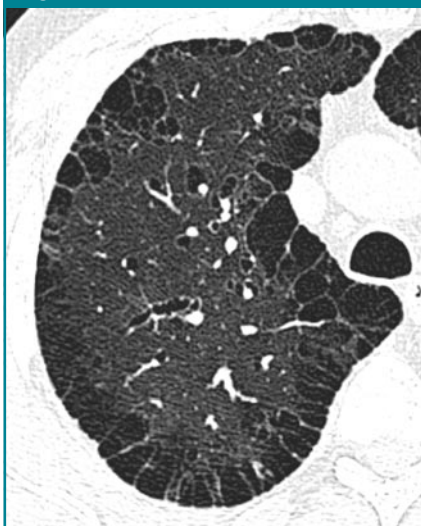
Figure 46

Figure 46: Transverse CT scan shows panacinar emphysema.

panacinar emphysema

Pathology.—Panacinar emphysema involves all portions of the acinus and secondary pulmonary lobule more or less uniformly (42). It predominates in the lower lobes and is the form of emphysema associated with α1-antitrypsin deficiency.

CT scans.—Panacinar emphysema manifests as a generalized decrease of the lung parenchyma with a decrease in the caliber of blood vessels in the affected lung (97,98) (Fig 46). Severe panacinar emphysema may coexist and merge with severe centrilobular emphysema. The appearance of featureless decreased attenuation may be indistinguishable from severe constrictive obliterative bronchiolitis (99). The term *panlobular emphysema* is synonymous. (See also *emphysema.*)

hinhanhykhoa.com

Figure 47: Transverse CT scan shows paraseptal emphysema.

paraseptal emphysema

Pathology.—Paraseptal emphysema is characterized by predominant involvement of the distal alveoli and their ducts and sacs. It is characteristically bounded by any pleural surface and the interlobular septa (42,43).

CT scans.—This emphysema is characterized by subpleural and peribronchovascular regions of low attenuation separated by intact interlobular septa (Fig 47), sometimes associated with bullae. The term *distal acinar emphysema* is synonymous. (See also *emphysema.*)

parenchyma

Anatomy.—Parenchyma refers to the gas-exchanging part of the lung, consisting of the alveoli and their capillaries.

Radiographs and CT scans.—The portion of the lung exclusive of visible pulmonary vessels and airways.
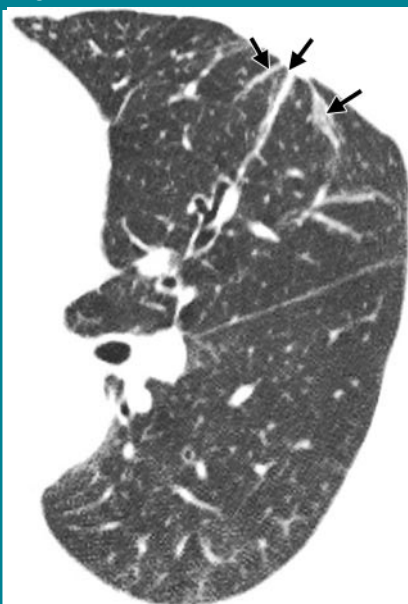
Figure 48: Transverse CT scan shows parenchymal bands (arrows).

parenchymal band

Radiographs and CT scans.—A parenchymal band is a linear opacity, usually 1–3 mm thick and up to 5 cm long that usually extends to the visceral pleura (which is often thickened and may be retracted at the site of contact) (Fig 48). It reflects pleuroparenchymal fibrosis and is usually associated with distortion of the lung architecture. Parenchymal bands are most frequently encountered in individuals who have been exposed to asbestos (100,101).

parenchymal opacification

Radiographs and CT scans.—Parenchymal opacification of the lungs may or may not obscure the margins of vessels and airway walls (45). *Consolidation* indicates that definition of these margins (excepting air bronchograms) is lost within the dense opacification, whereas *ground-glass opacity* indicates a smaller increase in attenuation, in which the definition of underlying structures is preserved (59). The more specific terms *consolidation* and *ground-glass opacity* are preferred. (See also *consolidation, ground-glass opacity.*)

peribronchovascular interstitium

Anatomy.—The peribronchovascular interstitium is a connective-tissue sheath that encloses the bronchi, pulmonary arteries, and lymphatic vessels. It extends from the hila to the lung periphery.

Figure 49: Transverse CT scan shows organizing pneumonia in a perilobular distribution (arrows).

perilobular distribution

Anatomy.—The perilobular region comprises the structures bordering the periphery of the secondary pulmonary lobule.

CT scans.—This pattern is characterized by distribution along the structures that border the pulmonary lobules (ie, interlobular septa, visceral pleura, and vessels) (102). The term is most frequently used in the context of diseases (eg, perilobular organizing pneumonia) that are distributed mainly around the inner surface of the secondary pulmonary lobule (103) (Fig 49). This may resemble indistinct thickening of the interlobular septa.

Figure 50: Transverse CT scan shows sarcoidosis with a perilymphatic distribution.

Figure 51: Transverse CT scan shows pleural plaque (arrow) anteriorly in right hemithorax.

Figure 52: Chest radiograph shows a pneumatocele (arrows).

perilymphatic distribution

Anatomy.—This pattern is characterized by distribution along or adjacent to the lymphatic vessels in the lung. The routes of lymphatics are found along bronchovascular bundles, in the interlobular septa, around larger pulmonary veins, and in the pleura; alveoli do not have lymphatics.

CT scans.—Abnormalities along the pathway of the pulmonary lymphatics— that is, in the perihilar, peribronchovascular, and centrilobular interstitium, as well as in the interlobular septa and subpleural locations— have a perilymphatic distribution (104). A perilymphatic distribution typically seen in sarcoidosis (Fig 50) and lymphangitic spread of cancer.
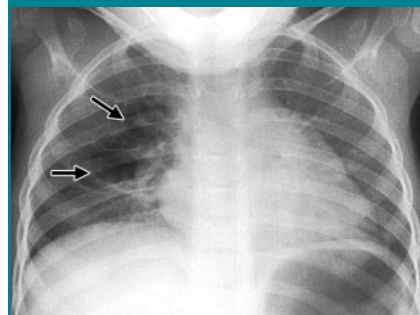
platelike atelectasis

See *linear atelectasis.*

pleural plaque

Pathology.—A pleural plaque is a fibrohyaline, relatively acellular lesion arising predominantly on the parietal pleural surface, particularly on the diaphragm and underneath ribs (105). Pleural plaques are almost invariably the consequence of previous (at least 15 years earlier) asbestos exposure.

Radiographs and CT scans.—Pleural plaques are well-demarcated areas of pleural thickening, seen as elevated flat or nodular lesions that often contain calcification (Fig 51). Plaques are of variable thickness, range from less than 1 to approximately 5 cm in diameter, and are more easily identified on CT scans than on chest radiographs (106). An en face plaque may simulate a pulmonary nodule on chest radiographs. (See also *pseudoplaque*.)

pneumatocele

Pathology.—A pneumatocele is a thin-walled, gas-filled space in the lung. It is most frequently caused by acute pneumonia, trauma, or aspiration of hydrocarbon fluid and is usually transient. The mechanism is believed to be a combination of parenchymal necrosis and check-valve airway obstruction (107).

Radiographs and CT scans.—A pneumatocele appears as an approximately round, thin-walled airspace in the lung (Fig 52).
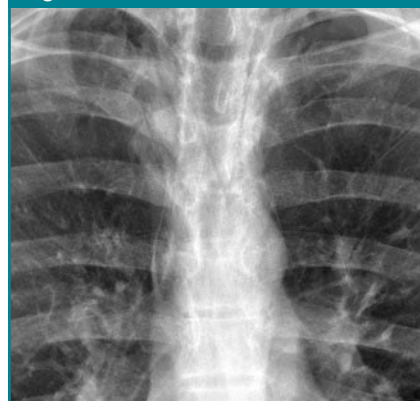
Figure 53: Magnified chest radiograph shows pneumomediastinum.

pneumomediastinum

Pathology.—Pneumomediastinum is the presence of gas in mediastinal tissue outside the esophagus and tracheobronchial tree. It may be caused by

spontaneous alveolar rupture, with subsequent tracking of air along the bronchovascular interstitium into the mediastinum. Pneumomediastinum is particularly associated with a history of asthma, severe coughing, or assisted ventilation.

Radiographs and CT scans.— Pneumomediastinum appears as lucent streaks on chest radiographs, mostly vertically oriented (Fig 53). Some of these streaks may outline vessels and main bronchi. (See also *pneumopericardium.*)

pneumonia

Pathology.—Pneumonia is inflammation of the airspaces and/or interstitium (eg, due to infection, as in bacterial pneumonia). Infective pneumonia is characterized by exudate resulting in consolidation. The term is also used to refer to a number of noninfectious disorders of the lung parenchyma characterized by varying degrees of inflammation and fibrosis (eg, idiopathic interstitial pneumonias) (5).
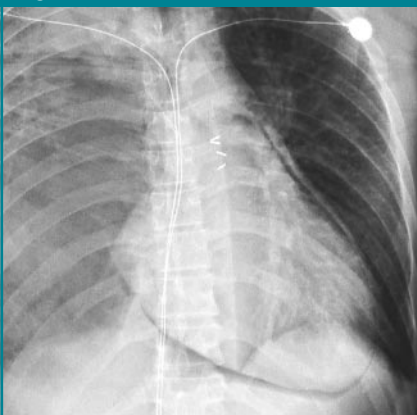
Figure 54

Figure 54: Chest radiograph shows pneumopericardium.

pneumopericardium

Pathology.—Pneumopericardium is the presence of gas in the pericardial space. It usually has an iatrogenic, often surgical, origin in adults.

Radiographs and CT scans.—Pneumopericardium is usually distinguish-

able from pneumomediastinum because the lucency (low attenuation) caused by air does not extend outside the pericardial sac (Fig 54). (See also *pneumomediastinum.*)

Figure 55

Figure 55: Chest radiograph shows pneumothorax.

pneumothorax and tension pneumothorax

Pathophysiology.—Pneumothorax refers to the presence of gas in the pleural space. Qualifiers include *spontaneous, traumatic, diagnostic,* and *tension.* Tension pneumothorax is the accumulation of intrapleural gas under pressure. In this situation, the ipsilateral lung will, if normal, collapse completely; however, a less than normally compliant lung may remain partially inflated.

Radiographs and CT scans.—On chest radiographs, a visceral pleural edge is visible (Fig 55) unless the pneumothorax is very small or the pleural edge is not tangential to the x-ray beam. Tension pneumothorax may be associated with considerable shift of the mediastinum and/or depression of the hemidiaphragm. Some shift can occur without tension because the pleural pressure in the presence of pneumothorax becomes atmospheric, while the pleural pressure in the contralateral hemithorax remains negative.

Figure 56
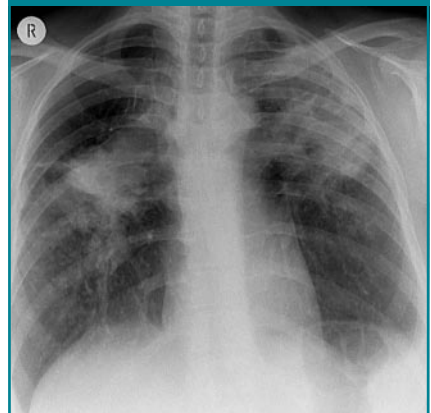
Figure 56: Chest radiograph shows bilateral progressive massive fibrosis.

progressive massive fibrosis

Pathology.—This condition is caused by slow-growing conglomeration of dust particles and collagen deposition in individuals (mostly coal workers) heavily exposed to inorganic dust (108).

Radiographs and CT scans.—Progressive massive fibrosis manifests as masslike lesions, usually bilateral and in the upper lobes (Fig 56). Background nodular opacities reflect accompanying pneumoconiosis, with or without emphysematous destruction adjacent to the massive fibrosis (109). Lesions similar to progressive massive fibrosis sometimes occur in other conditions, such as sarcoidosis and talcosis (109,110).

Radiology
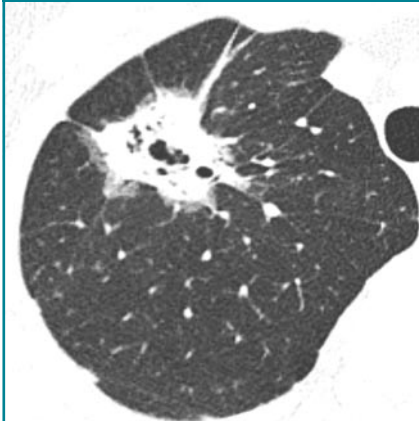
Figure 57

Figure 57: Transverse CT scan shows pseudo-cavitation in an adenocarcinoma.

pseudocavity

*CT scans.*—A pseudocavity appears as an oval or round area of low attenuation in lung nodules, masses, or areas of consolidation that represent spared parenchyma, normal or ectatic bronchi, or focal emphysema rather than cavitation. These pseudocavities usually measure less than 1 cm in diameter. They have been described in patients with adenocarcinoma (Fig 57), bronchioloalveolar carcinoma (111), and benign conditions such as infectious pneumonia.

Figure 58
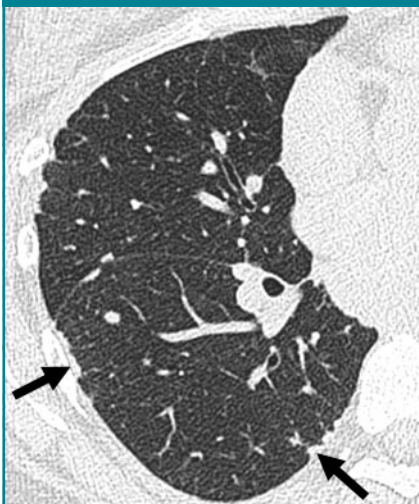
Figure 58: Transverse CT scan shows pseudoplaques (arrows) in a patient with sarcoidosis.

pseudoplaque

CT scans.—A pseudoplaque is a pulmonary opacity contiguous with the visceral pleura formed by coalescent small nodules. It simulates the appearance of a pleural plaque. This entity is encountered most commonly in sarcoidosis (Fig 58), silicosis, and coal-worker's pneumoconiosis (86).

Figure 59


Figure 59: Chest radiograph shows redistribution of blood flow to upper lung zones.

pulmonary blood flow redistribution

Pathophysiology.—Pulmonary blood flow redistribution refers to any departure from the normal distribution of blood flow in the lungs that is caused by an increase in pulmonary vascular resistance elsewhere in the pulmonary vascular bed.

Radiographs and CT scans.—Pulmonary blood flow redistribution is indicated by a decrease in the size and/or number of visible pulmonary vessels in one or more lung regions (Fig 59), with a corresponding increase in number and/or size of pulmonary vessels in other parts of the lung. Upper lobe blood diversion in patients with mitral valve disease is the archetypal example of redistribution (112,113).

Figure 60
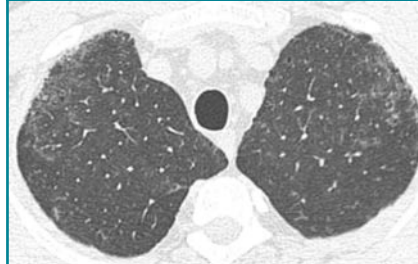
Figure 60: Transverse CT scan shows centrilobular micronodules and patchy ground-glass opacity typical of respiratory bronchiolitis–interstitial lung disease.

respiratory bronchiolitis–interstitial lung disease, or RB-ILD

Pathology.—RB-ILD is a smoking-related disease characterized by inflammation (predominantly by macrophages) of the respiratory bronchioles and peribronchiolar alveoli (5), sometimes with elements of or overlap with nonspecific and desquamative interstitial pneumonias (114).

CT scans.—RB-ILD typically manifests as extensive centrilobular micronodules and patchy ground-glass opacity corresponding to macrophage-rich alveolitis (Fig 60), with or without fine fibrosis (115,116). It is often accompanied by bronchial wall thickening and minor centrilobular emphysema. Areas of air trapping reflect a bronchiolitic component.

Figure 61

Figure 61: Chest radiograph shows reticular pattern.

Figure 62

Figure 62: Chest radiograph shows reticulonodular pattern.

reversed halo sign

CT scans.—The reversed halo sign is a focal rounded area of ground-glass opacity surrounded by a more or less complete ring of consolidation (Fig 63). A rare sign, it was initially reported to be specific for cryptogenic organizing pneumonia (117,118) but was subsequently described in patients with paracoccidioidomycosis (119). Similar to the halo sign, this sign will probably lose its specificity as it is recognized in other conditions. (See also *halo sign.*)

Figure 64

Figure 64: Magnified chest radiograph shows paratracheal stripe (arrows).

reticular pattern

Radiographs and CT scans.—On chest radiographs, a reticular pattern is a collection of innumerable small linear opacities that, by summation, produce an appearance resembling a net (synonym: *reticulation*) (Fig 61). This finding usually represents interstitial lung disease. The constituents of a reticular pattern are more clearly seen at thin-section CT, whether they are interlobular septal thickening, intralobular lines, or the cyst walls of honeycombing. (*Reticular pattern* and *honeycombing* should not be considered synonymous. See also *honeycombing.*)
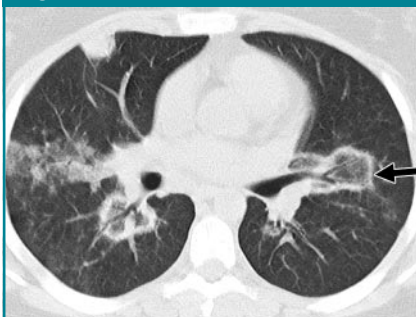
reticulonodular pattern

Radiographs and CT scans.—A combined reticular and nodular pattern, the reticulonodular pattern is usually the result of the summation of points of intersection of innumerable lines, creating the effect on chest radiographs of superimposed micronodules (Fig 62). The dimension of the nodules depends on the size and number of linear or curvilinear elements. (See also *reticular pattern.*) On CT scans, the pattern appears as a concurrence of reticular and micronodular patterns. The micronodules can be situated in the center of the reticular elements (eg, centrilobular micronodules) or superimposed on the linear opacities (eg, septal micronodules).

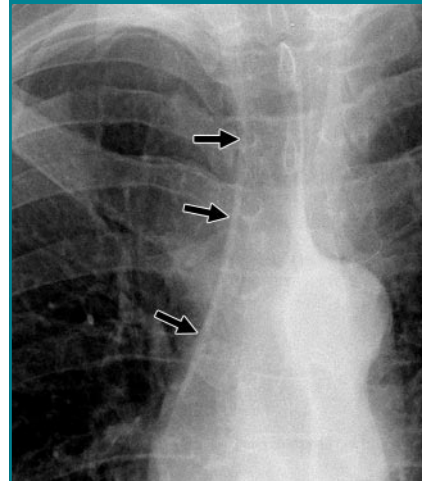### right paratracheal stripe

Anatomy and radiographs.—The right paratracheal stripe is a vertical, linear, soft-tissue opacity less than 4 mm wide. It corresponds to the right tracheal wall, contiguous mediastinal tissues, and adjacent pleura (Fig 64). The stripe is 3–4 cm in height and extends from approximately the level of the medial ends of the clavicles to the right tracheobronchial angle on a frontal chest radiograph (120). It is seen in up to 94% of adults but is widened or absent in individuals with abundant mediastinal fat. The commonest pathologic cause of widening, deformity, or obliteration of this stripe is paratracheal lymph node enlargement.

Figure 63

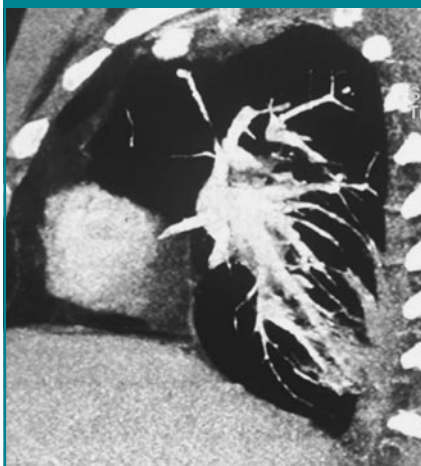**Figure 63:** Transverse CT scan shows reversed halo sign (arrow).

Figure 65

Figure 65: Sagittal CT scan shows rounded atelectasis in left lower lobe.

rounded atelectasis

Pathology.—Rounded atelectasis is rounded collapsed lung associated with invaginated fibrotic pleura and thickened and fibrotic interlobular septa. Most frequently, it is the consequence of an asbestos-induced exudative pleural effusion with resultant pleural scarring (121), but it may occur with any cause of pleural fibrosis.

Radiographs and CT scans.—On chest radiographs, rounded atelectasis appears as a mass abutting a pleural surface, usually in the posterior part of a lower lobe. Distorted vessels have a curvilinear disposition as they converge on the mass (the comet tail sign). The degree of lobar retraction depends on the volume of atelectatic lung. It is almost invariably associated with other signs of pleural fibrosis (eg, blunting of costophrenic angle). CT is more sensitive for the detection and display of the characteristic features of rounded atelectasis (122,123) (Fig 65). An additional sign is homogeneous uptake of contrast medium in the atelectatic lung. Synonyms include *folded lung syndrome, helical atelectasis, Blesovsky syndrome, pleural pseudotumor,* and *pleuroma.*

secondary pulmonary lobule

See *lobule.*

segment

Anatomy.—A segment is the unit of a lobe ventilated by a segmental bronchus, perfused by a segmental pulmonary artery, and drained by an intersegmental pulmonary vein. There are two to five segments per lobe.

Radiographs and CT scans.—Individual segments cannot be precisely delineated on chest radiographs and CT scans, and their identification is made inferentially on the basis of the position of the supplying segmental bronchus and artery. When occasionally present, intersegmental fissures help to identify segments.

septal line

See *interlobular septum.*

septal thickening
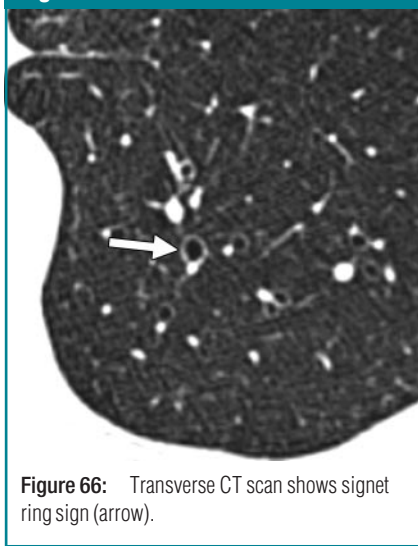
See *interlobular septal thickening.*

Figure 66

Figure 66: Transverse CT scan shows signet ring sign (arrow).

signet ring sign

CT scans.—This finding is composed of a ring-shaped opacity representing a dilated bronchus in cross section and a smaller adjacent opacity representing its pulmonary artery, with the combination resembling a signet (or pearl) ring (124) (Fig 66). It is the basic CT sign of bronchiectasis (27,125). The signet ring sign can also be seen in diseases charac-

terized by abnormal reduced pulmonary arterial flow (eg, proximal interruption of pulmonary artery [126] or chronic thromboembolism [127]). Occasionally, the tiny vascular opacity abutting a bronchus is a bronchial, rather than a pulmonary, artery.

Figure 67
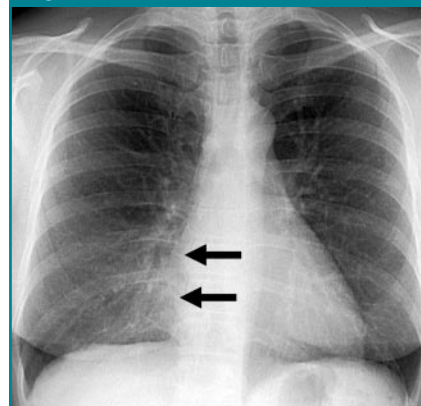
Figure 67: Chest radiograph shows silhouette sign, with obscuration of right border of heart (arrows).

silhouette sign

Radiographs.—The silhouette sign is the absence of depiction of an anatomic soft-tissue border. It is caused by consolidation and/or atelectasis of the adjacent lung (Fig 67), by a large mass, or by contiguous pleural fluid (128,129). The silhouette sign results from the juxtaposition of structures of similar radiographic attenuation. The sign actually refers to the absence of a silhouette. It is not always indicative of disease (eg, unexplained absence of right border of heart is seen in association with pectus excavatum and sometimes in healthy individuals).

small-airways disease

Pathology.—This phrase is an arbitrary term used more frequently in thin-section CT descriptions than in the pathophysiology literature, where it was first coined (130). *Small-airways disease* now generally refers to any condition affecting the bronchioles, whereas

bronchiolitis more specifically describes inflammation of the bronchioles (131).

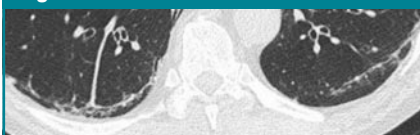*CT scans.*—Small airways are considered to be those with an internal diameter smaller than or equal to 2 mm and a normal wall thickness of less than 0.5 mm (32). Small-airways disease is manifest on CT scans as one or more of the following patterns: mosaic attenuation, air trapping, centrilobular micronodules, tree-in-bud pattern, or bronchiolectasis.


Figure 68: Transverse CT scan shows a subpleural curvilinear line.

subpleural curvilinear line

CT scans.—This finding is a thin curvilinear opacity, 1–3 mm in thickness, lying less than 1 cm from and parallel to the pleural surface (Fig 68). It corresponds to atelectasis of normal lung if seen in the dependent posteroinferior portion of lung of a patient in the supine position and is subsequently shown to disappear on CT sections acquired with the patient prone. It may also be encountered in patients with pulmonary edema (132) or fibrosis (other signs are usually present). Though described in the context of asbestosis, this finding is not specific for asbestosis.
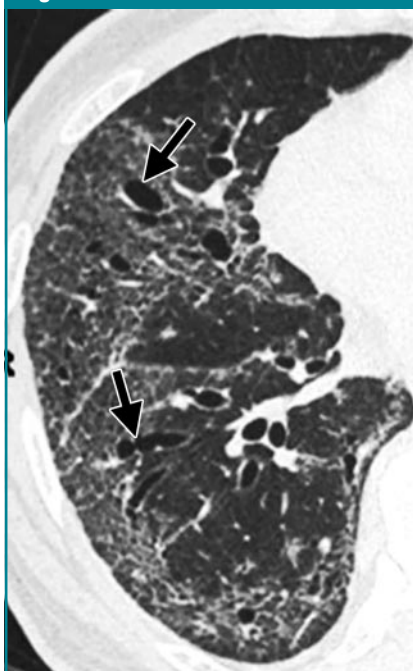
Figure 69: Transverse CT scan shows traction bronchiectasis (arrows) cased by retractile pulmonary fibrosis.

traction bronchiectasis and traction bronchiolectasis

CT scans.—Traction bronchiectasis and traction bronchiolectasis respectively represent irregular bronchial and bronchiolar dilatation caused by surrounding retractile pulmonary fibrosis (130). Dilated airways are usually identifiable as such (Fig 69) but may be seen as cysts (bronchi) or microcysts (bronchioles in the lung periphery). The juxtaposition of numerous cystic airways may make the distinction from "pure" fibrotic honeycombing difficult.
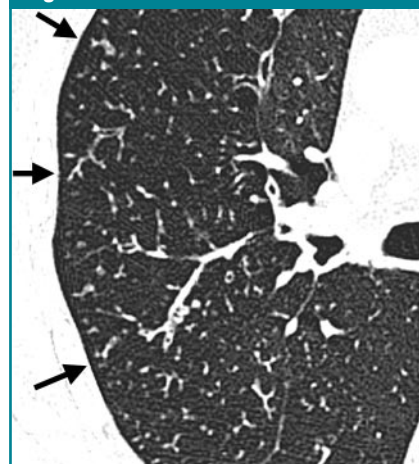
Figure 70: Transverse CT scan shows tree-in-bud pattern (arrows).

tree-in-bud pattern

CT scans.—The tree-in-bud pattern represents centrilobular branching structures that resemble a budding tree. The pattern reflects a spectrum of endo- and peribronchiolar disorders, including mucoid impaction, inflammation, and/or fibrosis (134,135) (Fig 70). This pattern is most pronounced in the lung periphery and is usually associated with abnormalities of the larger airways. It is particularly common in diffuse panbronchiolitis (136), endobronchial spread of mycobacterial infection (137), and cystic fibrosis. A similar pattern is a rare manifestation of arteriolar (microangiopathic) disease (138).

Figure 71
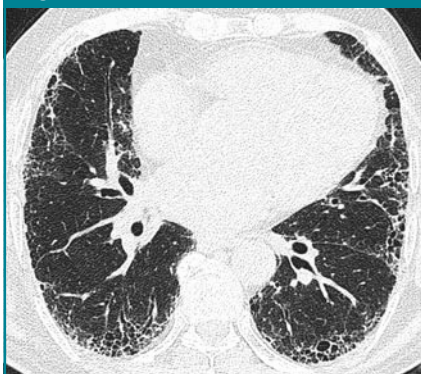
Figure 71: Transverse CT scan shows basal and subpleural honeycombing, indicative of usual interstitial pneumonia.

usual interstitial pneumonia, or UIP

Pathology.—UIP is a histologic pattern of pulmonary fibrosis characterized by temporal and spatial heterogeneity, with established fibrosis and honeycombing interspersed among normal lung. Fibroblastic foci with fibrotic destruction of lung architecture, often with honeycombing, are the key findings (5). The fibrosis is initially concentrated in the lung periphery. UIP is the pattern seen in idiopathic pulmonary fibrosis, but can be encountered in diseases of known cause (eg, some cases of chronic hypersensitivity pneumonitis).

Radiographs and CT scans.—Honeycombing with a basal and subpleural distribution (Fig 71) is regarded as pathognomonic (63,65), but not all cases of biopsy-proved UIP have this distinctive CT pattern.

References

1. Tuddenham WJ. Glossary of terms for thoracic radiology: recommendations of the Nomenclature Committee of the Fleischner Society. AJR Am J Roentgenol 1984;143: 509–517.

2. Austin JH, Müller NL, Friedman PJ, et al. Glossary of terms for CT of the lungs: recommendations of the Nomenclature Committee of the Fleischner Society. Radiology 1996;200:327–331.

3. Huth EJ. Medical style and format: an international manual for authors, editors, and publishers. Philadelphia, Pa: ISI, 1987;126. Cited by:Skryd PJ. Radiologic nomenclature and abbreviations. Radiology 2001; 218(1)10–11.

4. Webb WR. Thin-section CT of the secondary pulmonary lobule: anatomy and the image—the 2004 Fleischner lecture. Radiology 2006;239(2):322–338.

5. American Thoracic Society/European Respiratory Society International Multidisciplinary Consensus Classification of the Idiopathic Interstitial Pneumonias. This joint statement of the American Thoracic Society (ATS), and the European Respiratory Society (ERS) was adopted by the ATS board of directors, June 2001 and by the ERS executive committee, June 2001. Am J Respir Crit Care Med 2002;165:277–304. [Published correction appears in Am J Respir Crit Care Med 2002;166(3):426.]

6. Johkoh T, Müller NL, Taniguchi H, et al. Acute interstitial pneumonia: thin-section CT findings in 36 patients. Radiology 1999; 211:859–863.

7. Lynch DA, Travis WD, Müller NL, et al. Idiopathic interstitial pneumonias: CT features. Radiology 2005;236(1):10–21.

8. Reed JC, Madewell JE. The air bronchogram in interstitial disease of the lungs: a radiological-pathological correlation. Radiology 1975;116:1–9.

9. Buckingham SJ, Hansell DM. Aspergillus in the lung: diverse and coincident forms. Eur Radiol 2003;13:1786–1800.

10. Abramson S. The air crescent sign. Radiology 2001;218(1):230–232.

11. Arakawa H, Webb WR. Air trapping on expiratory high-resolution CT scans in the absence of inspiratory scan abnormalities: correlation with pulmonary function tests and differential diagnosis. AJR Am J Roentgenol 1998;170:1349–1353.

12. Bankier AA, Van Muylem A, Scillia P, De Maertelaer V, Estenne M, Gevenois PA. Air trapping in heart-lung transplant recipients: variability of anatomic distribution and extent at sequential expiratory thin-section CT. Radiology 2003;229: 737–742.

13. Arakawa H, Kurihara Y, Sasaka K, Nakajima Y, Webb WR. Air trapping on CT of patients with pulmonary embolism. AJR Am J Roentgenol 2002;178:1201–1207.

14. Murata K, Khan A, Herman PG. Pulmonary parenchymal disease: evaluation with high-resolution CT. Radiology 1989;170:629–635.

15. Heitzman ER. The infraaortic area. In: The mediastinum: radiologic correlations with anatomy and pathology. Berlin, Germany: Springer-Verlag, 1988;151:–168.

16. Blank N, Castellino RA. Patterns of pleural reflections of the left superior mediastinum: normal anatomy and distortions produced by adenopathy. Radiology 1972;102:585–589.

17. Im JG, Webb WR, Han MC, Park JH. Apical opacity associated with pulmonary tuberculosis: high-resolution CT findings. Radiology 1991;178:727–731.

18. Yousem SA. Pulmonary apical cap: a distinctive but poorly recognized lesion in pulmonary surgical pathology. Am J Surg Pathol 2001;25:679–683.

19. Dail DH. Pulmonary apical cap. Am J Surg Pathol 2001;25:1344.

20. Woodring JH, Reed JC. Types and mechanisms of pulmonary atelectasis. J Thorac Imaging 1996;11:92–108.

21. Molina PL, Hiken JN, Glazer HS. Imaging evaluation of obstructive atelectasis. J Thorac Imaging 1996;11:176–186.

22. Woodring JH, Reed JC. Radiographic manifestations of lobar atelectasis. J Thorac Imaging 1996;11:109–144.

23. Heitzman ER. The azygoesophageal recess. In: The mediastinum: radiologic correlations with anatomy and pathology. Berlin, Germany: Springer-Verlag, 1988;276:–286.

24. Ren H, Hruban RH, Kuhlman JE, et al. Computed tomography of inflation-fixed lungs: the beaded septum sign of pulmonary metastases. J Comput Assist Tomogr 1989;13:411–416.

25. Ryu JH, Swensen SJ. Cystic and cavitary lung diseases: focal and diffuse. Mayo Clin Proc 2003;78:744–752.

26. Kang EY, Miller RR, Müller NL. Bronchiectasis: comparison of preoperative thin-section CT and pathologic findings in resected specimens. Radiology 1995; 195:649–654.

27. Naidich DP, McCauley DI, Khouri NF, Stitik FP, Siegelman SS. Computed tomography of bronchiectasis. J Comput Assist Tomogr 1982;6:437–444.

28. Grenier P, Maurice F, Musset D, Menu Y, Nahum H. Bronchiectasis: assessment by thin-section CT. Radiology 1986;161:95–99.

29. Dodd JD, Souza CA, Müller NL. Conventional high-resolution CT versus helical high-resolution MDCT in the detection of bronchiectasis. AJR Am J Roentgenol 2006; 187:414–420.

30. Hansen JE, Ampaya PE, Bryant GH, Navin JJ. Branching pattern of airways and airspaces of single human terminal bronchiole. J Appl Physiol 1975;38:983–989.

31. Buckley CE, Tucker DH, Thorne NA, Sieker HO. Bronchiolectasis: the clinical syndrome and its relationship to chronic lung disease. Am J Med 1965;38:190–198.

32. Hansell DM. Small airways diseases: detection and insights with computed tomography. Eur Respir J 2001;17:1294–1313.

33. Myers JL, Colby TV. Pathologic manifestations of bronchiolitis, constrictive bronchiolitis, cryptogenic organizing pneumonia, and diffuse panbronchiolitis. Clin Chest Med 1993;14:611–622.

34. Woodring JH. Unusual radiographic manifestations of lung cancer. Radiol Clin North Am 1990;28:599–618.

35. Müller NL, Kullnig P, Miller RR. The CT findings of pulmonary sarcoidosis: analysis of 25 patients. AJR Am J Roentgenol 1989; 152:1179–1182.

36. Huang L, Schnapp LM, Gruden JF, Hopewell PC, Stansell JD. Presentation of AIDS-related pulmonary Kaposi's sarcoma diagnosed by bronchoscopy. Am J Respir Crit Care Med 1996;153:1385–1390.

37. Oikonomou A, Hansell DM. Organizing pneumonia: the many morphological faces. Eur Radiol 2002;12:1486–1496.

38. Seo JB, Song KS, Lee JS, et al. Broncholithiasis: review of the causes with radiologic-pathologic correlation. RadioGraphics 2002;22(Spec Issue):S199–S213.

39. Murata K, Itoh H, Todo G, et al. Centrilobular lesions of the lung: demonstration by high-resolution CT and pathologic correlation. Radiology 1986;161:641–645.

40. Heitzman ER, Markarian B, Berger I, Dailey E. The secondary pulmonary lobule: a practical concept for interpretation of chest radiographs. I. Roentgen anatomy of the normal secondary pulmonary lobule. Radiology 1969;93:507–512.

41. Webb WR, Stein MG, Finkbeiner WE, Im JG, Lynch D, Gamsu G. Normal and diseased isolated lungs: high-resolution CT. Radiology 1988;166:81–87.

42. The definition of emphysema. Report of a National Heart, Lung, and Blood Institute, Division of Lung Diseases workshop. Am Rev Respir Dis 1985;132:182–185.

43. Thurlbeck WM, Müller NL. Emphysema: definition, imaging, and quantification. AJR Am J Roentgenol 1994;163:1017–1025.

44. Foster WL Jr, Pratt PC, Roggli VL, Godwin JD, Halvorsen RA Jr, Putman CE. Centrilobular emphysema: CT-pathologic correlation. Radiology 1986;159:27–32.

45. Leung AN, Miller RR, Müller NL. Parenchymal opacification in chronic infiltrative lung diseases: CT-pathologic correlation. Radiology 1993;188:209–214.

46. Laurent F, Philippe JC, Vergier B, et al. Exogenous lipoid pneumonia: HRCT, MR, and pathologic findings. Eur Radiol 1999;9: 1190–1196.

47. Kuhlman JE, Scatarige JC, Fishman EK, Zerhouni EA, Siegelman SS. CT demonstration of high attenuation pleural-parenchymal lesions due to amiodarone therapy. J Comput Assist Tomogr 1987;11:160–162.

48. Murch CR, Carr DH. Computed tomography appearances of pulmonary alveolar proteinosis. Clin Radiol 1989;40:240–243.

49. Rossi SE, Erasmus JJ, Volpacchio M, Franquet T, Castiglioni T, McAdams HP. "Crazy-paving" pattern at thin-section CT of the lungs: radiologic-pathologic overview. RadioGraphics 2003;23:1509–1519.

50. Franquet T, Gimenez A, Bordes R, Rodriguez-Arias JM, Castella J. The crazy-paving pattern in exogenous lipoid pneumonia: CT-pathologic correlation. AJR Am J Roentgenol 1998;170:315–317.

51. Genereux GP. The end-stage lung: pathogenesis, pathology, and radiology. Radiology 1975;116:279–289.

52. Aberle DR, Hansell DM, Brown K, Tashkin DP. Lymphangiomyomatosis: CT, chest radiographic, and functional correlations. Radiology 1990;176:381–387.

53. Moore AD, Godwin JD, Müller NL, et al. Pulmonary histiocytosis X: comparison of radiographic and CT findings. Radiology 1989;172:249–254.

54. Primack SL, Hartman TE, Hansell DM, Müller NL. End-stage lung disease: CT findings in 61 patients. Radiology 1993;189: 681–686.

55. Hartman TE, Primack SL, Swensen SJ, Hansell D, McGuinness G, Müller NL. Desquamative interstitial pneumonia: thin-section CT findings in 22 patients. Radiology 1993;187:787–790.

56. Lang MR, Fiaux GW, Gillooly M, Stewart JA, Hulmes DJ, Lamb D. Collagen content of alveolar wall tissue in emphysematous and non-emphysematous lungs. Thorax 1994;49:319–326.

57. Cardoso WV, Sekhon HS, Hyde DM, Thurlbeck WM. Collagen and elastin in human pulmonary emphysema. Am Rev Respir Dis 1993;147:975–981.

58. Foster WL Jr, Gimenez EI, Roubidoux MA, et al. The emphysemas: radiologic-pathologic correlations. RadioGraphics 1993;13: 311–328.

59. Remy-Jardin M, Remy J, Giraud F, Wattinne L, Gosselin B. Computed tomography (CT) assessment of ground-glass opacity: semiology and significance. J Thorac Imaging 1993;8:249–264.

60. Remy-Jardin M, Giraud F, Remy J, Copin MC, Gosselin B, Duhamel A. Importance of ground-glass attenuation in chronic diffuse infiltrative lung disease: pathologic-CT correlation. Radiology 1993;189:693–698.

61. Kuhlman JE, Fishman EK, Siegelman SS. Invasive pulmonary aspergillosis in acute leukemia: characteristic findings on CT, the CT halo sign, and the role of CT in early diagnosis. Radiology 1985;157:611–614.

62. Primack SL, Hartman TE, Lee KS, Müller NL. Pulmonary nodules and the CT halo sign. Radiology 1994;190:513–515.

63. Lynch DA, David GJ, Safrin S, et al. High-resolution computed tomography in idiopathic pulmonary fibrosis: diagnosis and prognosis. Am J Respir Crit Care Med 2005;172:488–493.

64. American Thoracic Society. Idiopathic pulmonary fibrosis: diagnosis and treatment: international consensus statement—American Thoracic Society (ATS), and the European Respiratory Society (ERS). Am J Respir Crit Care Med 2000;161(2 pt 1): 646–664.

65. Hunninghake GW, Lynch DA, Galvin JR, et al. Radiologic findings are strongly associated with a pathologic diagnosis of usual interstitial pneumonia. Chest 2003;124: 1215–1223.

66. Misumi S, Lynch DA. Idiopathic pulmonary fibrosis/usual interstitial pneumonia: imaging diagnosis, spectrum of abnormalities, and temporal progression. Proc Am Thorac Soc 2006;3:307–314.

67. Dalen JE, Haffajee CI, Alpert JS III, Howe JP, Ockene IS, Paraskos JA. Pulmonary embolism, pulmonary hemorrhage and pulmonary infarction. N Engl J Med 1977;296: 1431–1435.

68. Ren H, Kuhlman JE, Hruban RH, Fishman EK, Wheeler PS, Hutchins GM. CT of inflation-fixed lungs: wedge-shaped density and

vascular sign in the diagnosis of infarction. J Comput Assist Tomogr 1990;14:82–86.

69. Patterson HS, Sponaugle DN. Is infiltrate a useful term in the interpretation of chest radiographs? physician survey results. Radiology 2005;235(1):5–8.

70. Kang EY, Grenier P, Laurent F, Müller NL. Interlobular septal thickening: patterns at high-resolution computed tomography. J Thorac Imaging 1996;11:260–264.

71. Kemper AC, Steinberg KP, Stern EJ. Pulmonary interstitial emphysema: CT findings. AJR Am J Roentgenol 1999;172:1642.

72. Donnelly LF, Lucaya J, Ozelame V, et al. CT findings and temporal course of persistent pulmonary interstitial emphysema in neonates: a multiinstitutional study. AJR Am J Roentgenol 2003;180:1129–1133.

73. Weibel ER. Looking into the lung: what can it tell us? AJR Am J Roentgenol 1979;133:1021–1031.

74. Kattan KR, Eyler WR, Felson B. The juxtaphrenic peak in upper lobe collapse. Radiology 1980;134:763–765.

75. Cameron DC. The juxtaphrenic peak (Katten's sign) is produced by rotation of an inferior accessory fissure. Australas Radiol 1993;37:332–335.

76. Davis SD, Yankelevitz DF, Wand A, Chiarella DA. Juxtaphrenic peak in upper and middle lobe volume loss: assessment with CT. Radiology 1996;198:143–149.

77. Westcott JL, Cole S. Plate atelectasis. Radiology 1985;155:1–9.

78. Miller WS. The lung. 2nd ed. Springfield, Ill: Thomas, 1947;203:–205.

79. Glazer GM, Gross BH, Quint LE, Francis IR, Bookstein FL, Orringer MB. Normal mediastinal lymph nodes: number and size according to American Thoracic Society mapping. AJR Am J Roentgenol 1985;144:261–265.

80. Remy-Jardin M, Duyck P, Remy J, et al. Hilar lymph nodes: identification with spiral CT and histologic correlation. Radiology 1995;196:387–394.

81. Swigris JJ, Berry GJ, Raffin TA, Kuschner WG. Lymphoid interstitial pneumonia: a narrative review. Chest 2002;122:2150–2164.

82. Johkoh T, Müller NL, Pickford HA, et al. Lymphocytic interstitial pneumonia: thin-section CT findings in 22 patients. Radiology 1999;212:567–572.

83. Ichikawa Y, Kinoshita M, Koga T, Oizumi K, Fujimoto K, Hayabuchi N. Lung cyst formation in lymphocytic interstitial pneumonia: CT features. J Comput Assist Tomogr 1994;18:745–748.

84. Heitzman ER. The mediastinum: radiologic correlations with anatomy and pathology. Berlin, Germany: Springer-Verlag, 1988;7:–309.

85. Fraser RS, Müller NL, Colman N, Paré PD. The mediastinum: diagnosis of diseases of the chest. 4th ed. Philadelphia, Pa: Saunders, 1999;205:–211.

86. Remy-Jardin M, Beuscart R, Sault MC, Marquette CH, Remy J. Subpleural micronodules in diffuse infiltrative lung diseases: evaluation with thin-section CT scans. Radiology 1990;177:133–139.

87. Remy-Jardin M, Remy J, Wallaert B, Müller NL. Subacute and chronic bird breeder hypersensitivity pneumonitis: sequential evaluation with CT and correlation with lung function tests and bronchoalveolar lavage. Radiology 1993;189:111–118.

88. Brauner MW, Lenoir S, Grenier P, Cluzel P, Battesti JP, Valeyre D. Pulmonary sarcoidosis: CT assessment of lesion reversibility. Radiology 1992;182:349–354.

89. Worthy SA, Müller NL, Hartman TE, Swensen SJ, Padley SP, Hansell DM. Mosaic attenuation pattern on thin-section CT scans of the lung: differentiation among infiltrative lung, airway, and vascular diseases as a cause. Radiology 1997;205:465–470.

90. Martin KW, Sagel SS, Siegel BA. Mosaic oligemia simulating pulmonary infiltrates on CT. AJR Am J Roentgenol 1986;147:670–673.

91. Arakawa H, Webb WR, McCowin M, Katsou G, Lee KN, Seitz RF. Inhomogeneous lung attenuation at thin-section CT: diagnostic value of expiratory scans. Radiology 1998;206:89–94.

92. Hansell DM, Wells AU, Rubens MB, Cole PJ. Bronchiectasis: functional significance of areas of decreased attenuation at expiratory CT. Radiology 1994;193:369–374.

93. Roberts CM, Citron KM, Strickland B. Intrathoracic aspergilloma: role of CT in diagnosis and treatment. Radiology 1987;165:123–128.

94. Erasmus JJ, Connolly JE, McAdams HP, Roggli VL. Solitary pulmonary nodules. I. Morphologic evaluation for differentiation of benign and malignant lesions. RadioGraphics 2000;20:43–58.

95. MacDonald SL, Rubens MB, Hansell DM, et al. Nonspecific interstitial pneumonia and usual interstitial pneumonia: comparative appearances at and diagnostic accuracy of thin-section CT. Radiology 2001;221:600–605.

96. Lee KS, Kullnig P, Hartman TE, Müller NL. Cryptogenic organizing pneumonia: CT findings in 43 patients. AJR Am J Roentgenol 1994;162:543–546.

97. Guest PJ, Hansell DM. High resolution computed tomography in emphysema associated with alpha-1-antitrypsin deficiency. Clin Radiol 1992;45:260–266.

98. Spouge D, Mayo JR, Cardoso W, Müller NL. Panacinar emphysema: CT and pathologic findings. J Comput Assist Tomogr 1993;17:710–713.

99. Copley SJ, Wells AU, Müller NL, et al. Thin-section CT in obstructive pulmonary disease: discriminatory value. Radiology 2002;223:812–819.

100. Akira M, Yamamoto S, Yokoyama K, et al. Asbestosis: high-resolution CT—pathologic correlation. Radiology 1990;176:389–394.

101. Akira M, Yamamoto S, Inoue Y, Sakatani M. High-resolution CT of asbestosis and idiopathic pulmonary fibrosis. AJR Am J Roentgenol 2003;181:163–169.

102. Johkoh T, Müller NL, Ichikado K, Nakamura H, Itoh H, Nagareda T. Perilobular pulmonary opacities: high-resolution CT findings and pathologic correlation. J Thorac Imaging 1999;14:172–177.

103. Ujita M, Renzoni EA, Veeraraghavan S, Wells AU, Hansell DM. Organizing pneumonia: perilobular pattern at thin-section CT. Radiology 2004;232:757–761.

104. Colby TV, Swensen SJ. Anatomic distribution and histopathologic patterns in diffuse lung disease: correlation with HRCT. J Thorac Imaging 1996;11:1–26.

105. Roberts GH. The pathology of parietal pleural plaques. J Clin Pathol 1971;24:348–353.

106. Lynch DA, Gamsu G, Aberle DR. Conventional and high-resolution computed tomography in the diagnosis of asbestos-related diseases. RadioGraphics 1989;9:523–551.

107. Quigley MJ, Fraser RS. Pulmonary pneumatocele: pathology and pathogenesis. AJR Am J Roentgenol 1988;150:1275–1277.

108. Wagner JC, Wusteman FS, Edwards JH, Hill RJ. The composition of massive lesions in coal miners. Thorax 1975;30:382–388.

109. Chong S, Lee KS, Chung MJ, Han J, Kwon OJ, Kim TS. Pneumoconiosis: comparison of imaging and pathologic findings. RadioGraphics 2006;26:59–77.

110. Ward S, Heyneman LE, Reittner P, Kaze-

rooni EA, Godwin JD, Müller NL. Talcosis associated with IV abuse of oral medications: CT findings. AJR Am J Roentgenol 2000;174:789–793.

111. Weisbrod GL, Chamberlain D, Herman SJ. Cystic change (pseudocavitation) associated with bronchioloavleolar carcinoma: a report of four patients. J Thorac Imaging 1995;10:106–111.

112. Simon M. The pulmonary veins in mitral stenosis. J Fac Radiol 1958;9:25–32.

113. Milne EN. Physiological interpretation of the plain radiograph in mitral stenosis, including a review of criteria for the radiological estimation of pulmonary arterial and venous pressures. Br J Radiol 1963;36: 902–913.

114. Fraig M, Shreesha U, Savici D, Katzenstein AL. Respiratory bronchiolitis: a clinicopathologic study in current smokers, ex-smokers, and never-smokers. Am J Surg Pathol 2002;26:647–653.

115. Heyneman LE, Ward S, Lynch DA, Remy-Jardin M, Johkoh T, Müller NL. Respiratory bronchiolitis, respiratory bronchiolitis-associated interstitial lung disease, and desquamative interstitial pneumonia: different entities or part of the spectrum of the same disease process? AJR Am J Roentgenol 1999;173:1617–1622.

116. Hansell DM, Nicholson AG. Smoking-related diffuse parenchymal lung disease: HRCT-pathologic correlation. Semin Respir Crit Care Med 2003;24:377–392.

117. Zompatori M, Poletti V, Battista G, Diegoli M. Bronchiolitis obliterans with organizing pneumonia (BOOP), presenting as a ring-shaped opacity at HRCT (the atoll sign): a case report. Radiol Med (Torino) 1999;97: 308–310.

118. Kim SJ, Lee KS, Ryu YH, et al. Reversed halo sign on high-resolution CT of crypto-genic organizing pneumonia: diagnostic implications. AJR Am J Roentgenol 2003;180: 1251–1254.

119. Gasparetto EL, Escuissato DL, Davaus T, et al. Reversed halo sign in pulmonary paracoccidioidomycosis. AJR Am J Roentgenol 2005;184:1932–1934.

120. Savoca CJ, Austin JH, Goldberg HI. The right paratracheal stripe. Radiology 1977; 122:295–301.

121. Cohen AM, Crass JR, Chung-Park M, Tomashefski JF Jr. Rounded atelectasis and fibrotic pleural disease: the pathologic continuum. J Thorac Imaging 1993;8:309–312.

122. Lynch DA, Gamsu G, Ray CS, Aberle DR. Asbestos-related focal lung masses: manifestations on conventional and high-resolution CT scans. Radiology 1988;169:603–607.

123. O'Donovan PB, Schenk M, Lim K, Obuchowski N, Stoller JK. Evaluation of the reliability of computed tomographic criteria used in the diagnosis of round atelectasis. J Thorac Imaging 1997;12:54–58.

124. Ouellette H. The signet ring sign. Radiology 1999;212:67–68.

125. McGuinness G, Naidich DP, Leitman BS, McCauley DI. Bronchiectasis: CT evaluation. AJR Am J Roentgenol 1993;160:253–259.

126. Ryu DS, Spirn PW, Trotman-Dickenson B, et al. HRCT findings of proximal interruption of the right pulmonary artery. J Thorac Imaging 2004;19:171–175.

127. Remy-Jardin M, Remy J, Louvegny S, Artaud D, Deschildre F, Duhamel A. Airway changes in chronic pulmonary embolism: CT findings in 33 patients. Radiology 1997; 203:355–360.

128. Felson B, Felson H. Localisation of intrathoracic lesions by means of the postero-ante-rior roentgenogram: the silhouette sign. Radiology 1950;55:363–374.

129. Marshall GB, Farnquist BA, MacGregor JH, Burrowes PW. Signs in thoracic imaging. J Thorac Imaging 2006;21:76–90.

130. Hogg JC, Macklem PT, Thurlbeck WM. Site and nature of airway obstruction in chronic obstructive lung disease. N Engl J Med 1968;278:1355–1360.

131. Müller NL, Miller RR. Diseases of the bronchioles: CT and histopathologic findings. Radiology 1995;196:3–12.

132. Arai K, Takashima T, Matsui O, Kadoya M, Kamimura R. Transient subpleural curvilinear shadow caused by pulmonary congestion. J Comput Assist Tomogr 1990;14:87–88.

133. Desai SR, Wells AU, Rubens MB, Du Bois RM, Hansell DM. Traction bronchiectasis in cryptogenic fibrosing alveolitis: associated computed tomographic features and physiological significance. Eur Radiol 2003; 13:1801–1808.

134. Aquino SL, Gamsu G, Webb WR, Kee ST. Tree-in-bud pattern: frequency and significance on thin section CT. J Comput Assist Tomogr 1996;20:594–599.

135. Eisenhuber E. The tree-in-bud sign. Radiology 2002;222:771–772.

136. Akira M, Kitatani F, Yong-Sik L, et al. Diffuse panbronchiolitis: evaluation with high-resolution CT. Radiology 1988;168:433–438.

137. Im JG, Itoh H, Shim YS, et al. Pulmonary tuberculosis: CT findings—early active disease and sequential change with antituberculous therapy. Radiology 1993;186:653–660.

138. Franquet T, Gimenez A, Prats R, Rodriguez-Arias JM, Rodriguez C. Thrombotic microangiopathy of pulmonary tumors: a vascular cause of tree-in-bud pattern on CT. AJR Am J Roentgenol 2002;179:897–899.

hinhanhykhoa.com